Spatiotemporal Variability: Process-Independent Analysis of Printing Uniformity

by Saleh A. Abdel Motaal

A thesis submitted in partial fulfillment of the requirements
for the degree of Master of Science in the School of Print Media
in the College of Imaging Arts and Sciences
of the Rochester Institute of Technology

May 2014

Primary Thesis Advisor: Professor Christopher Bondy
Secondary Thesis Advisor: Professor Franz Sigg
Technical Consultant: Professor Michael Riordan

Acknowledgments

None of this would have been possible without the endless advice and insights from my mother who was instrumental to my success in all my studies. To everyone that helped me complete this work, thank you for all your support. It is not possible to adequately mention all the great people that made it possible to complete this lengthy study, especially my entire family.

With two great mentors, Professor Franz Sigg and Professor Christopher Bondy, my experience at the Rochester Institute of Technology (RIT) has changed my perspective on empowered me to follow through on one of the most challenging topics if the realm of printing quality. Another great mentor is Professor Michael Riordan who has work diligently with me on planning and guided me through this and other projects.

The Printing Uniformity framework was developed over a few years with the continued contributions of Professor Sigg that made it possible to iteratively refine concepts and develop the formulae with great patience. I thank Professors Patricia Sorce, Bruce Myers, and, Scott Williams for the help during the early stages of the work, and thank Professor Bondy for his limitless support and mentoring in the last two years.

The pressruns were conducted at the Printing Applications Laboratory (PAL) at RIT with paper donations from SAPPI. I must also acknowledge the amazing students and their instructor John Eldridge in the Printing Technology class who elected to use their time on the press to print some of the samples with diligence and care. Barbra Giordano, Frank White, at the PAL, as well as, Jennifer Ariza, John Dettmer, Daniel Gramlich, and Jeremy Vanslette, for producing the print samples, and, David Niles at SAPPI for supplying the paper; my sincere thanks to all.

I must also acknowledging my friends and mentors who guided me through complex theoretical and application challenges, Dr. Stephen Bloom, Dr. Ed Granger, John Seymour, Thomas Sprintzing, Dr. Stephen Viggiano and Dr. Eric Zeise. I also must acknowledge Laila Ramadan for her support that made allowed me to continue my work regardless of the challenges from the interesting events back home, in Egypt.

Table of Contents

List of Tables

List of Figures

List of Abbreviations

ISO	International Standards Organization
NPES	Association for Suppliers of Printing, Publishing and Converting Technologies (formerly known as National Printing Equipment Association)
CGATS	Committee for Graphic Arts Technologies Standards
CIE	Commission internationale de l'éclairage (translates to International Commission on Illumination)
CIEXYZ	CIE 1931 XYZ color space
CIELAB	CIE 1976 L*a*b* color space
IDEAlliance	International Digital Enterprise Alliance
GRACoL	General Requirements for Applications in Commercial Offset Lithography
SNAP	Specifications for Newsprint Advertising Production
SWOP	Specifications for Web Offset Publications
PET	Positron Emission Tomography.

List of Symbols

$v\Delta$ / $v\mathrm{K}$	Overall inaccuracy and imprecision values, page 37.
$v\delta_{\#}$ / $v\kappa_{\#}$	Regional inaccuracy and imprecision values indicating position, page 37.
Δ / K	Overall inaccuracy and imprecision scores, page 38.
$\delta_{\#}$ / $\kappa_{\#}$	Regional inaccuracy and imprecision scores indicating position, page 38.
$d\Delta_{\#}$ / $d\mathrm{K}_{\#}$	Overall inaccuracy and imprecision directionalities indicating direction, page 41.
$p\delta_{\#}$ / $p\kappa_{\#}$	Regional inaccuracy and imprecision proportions indicating position, page 39.
$f\mathrm{K}_{\mathrm{T}}$ / $f\mathrm{K}_{\mathrm{E}}$	Overall temporal and spatial factors, page 40.
D	ISO visual density value for black or Status T when indicated, page 42.

Abstract

This work explores printing uniformity from a quality standpoint. The study proposes a conceptual framework, quantitative models and a testing method for the measurement and analysis of printing uniformity independent from the printing process and press design. The proposed framework encompasses construct and indicators concerning the printing accuracy and printing precision dimensions of uniformity. The proposed models are derived for each of the indicators in the framework comprising a cohesive set of device- and process-independent image quality metrics (IQMs) for benchmarking and evaluating the spatial-temporal uniformity of printing systems relative to standard industry tolerances. The proposed test method builds on prior efforts on the same topic and borrows from and improves upon related studies by various authors.

Printing uniformity in this work is defined as the theoretical attribute that reflects the extent of variability for a given press. It has significant implications on a range of standards and specifications dealing with process control. This addresses a fundamental challenge in understanding variability in printing rather than focus on cause-effect relationships.

The literature revealed that some aspects of the topic are underexplored with the majority of the works addressing either the spatial or temporal domains independently. Additionally, parallel efforts were found with disparate terminologies, which made it hard to find clear definitions to concepts central to the topic.

Five press tests were conducted following the proposed method to help refine the concepts and metrics. They included three presses, including offset lithography and electrophotography. The findings were inline with findings from related studies, showing similarities and differences between printing units, presses, and processes

This work can serve as template for exploring phenomena using the triple-tiered approach for devising the concepts, models and methods. Future research on the uniformity of numerous printing systems across processes may provide great value in our understanding printing uniformity. Comprehensive testing across systems and processes creates opportunities for validating or refuting assumptions, which would ensure continuous improvement of quality control practices and ultimately better color consistency in printing.

Chapter 1
Introduction

With continuous advancements in color reproduction technology consumers of media have grown accustomed to vibrant and expressive matter in print and electronic media. In recent years, the graphic arts industry has seen exponential leaps in quality control systems. Whether it is a product over a shelf, a picture of that product in a catalog, a billboard or television advertisement, or the product page on web, consumers have a fine aptitude for sensing non-uniformities. Any discernible inconsistencies can quickly render a perception of distrust for the brand. At the same time, our appreciation for high quality can render an attraction to the brand and improve competitiveness.

Competition progressively heightens the expectations of the consumer regarding quality, including image quality. This requires continuous improvement in quality control practices, primarily, defining better process aims and tolerances. The front-and-center to achieving those goals lies in the understanding of variability and the breakdown of cause-effect relationships, which improve monitoring and facilitate more timely corrective action. The industry invests tremendous efforts on determining cause-effect relationships than on the understanding of variability, which is the main focus of this research.

As with any process, printing is subject to certain levels of variability that may result in color shift noticeable by the end user. Printing uniformity, from a quality control perspective, can be defined as a theoretical attribute that reflects the extent of variability in a given printing system. This attribute can have significant implications on the range of standards and specifications dealing with process control.

The objective of this research is to explore printing uniformity as it relates to image quality. The focus is on measuring and comparing the uniformity capabilities of printing systems relative to the reproduced image and independent from the printing process and the design of the system. This work begins by addressing a fundamental challenge in understanding variability in printing, laying foundations for research on cause-effect, process aims, and, ultimately, in the future, development of plausible psychophysical metrics for end user perception.

1.1. Background and Rationale

In printing, quality is addressed through international standards that define aim points and tolerances, and specifications that provide guidelines for the different printing applications. Specifications define criteria for conformance to the standards to meet the specific needs of different printing processes, substrates and colorants. For instance, the inks used in flexographic printing on polymer substrates, large format inkjets on vinyl and lithography or xerography on paper stock, each prescribe formulations optimized for the process and for the transfer and adherence of the image onto the substrate.

Specifications also address the specific needs of different end users and end use requirements. For instance, viewing distance will prescribe resolution parameters that are optimized to a reader's naked eye in close proximity, or, to approaching commuters, near or far. Similarly, viewing conditions and ambient lighting will also prescribe color and visual parameters optimized for bright daylight or at night, indoors or alongside the road.

Additionally, specifications provide mechanisms for print quality control. The main idea is to print measurable control elements in the outer slug region, as illustrated in *Figure 1*, to control the printing process. Color bars are used for controlling the accuracy of the color. They provide proxy measures for the color in the actual image and allow the operator to gauge the flow of ink during the run but then they are discarded after printing.

Figure 1. Sample offset lithography press sheet with a tail-edge color bar.

Printing uniformity has a fundamental implication not only on the refinement of process aims, but more so on the merit of these proxy measures to a point that ensures that the printed product will conform as indicated by the color bar for every press. While the knowledgebase on printing uniformity is rich in many aspects, an extensive review of the pertinent literature revealed that some aspects are simply underexplored.

With the printing industry poised at an unprecedented level of quality control and the increased diversity in printing technologies as well as the ever-expanding range of print formats, it is now time to take a deeper look into printing uniformity and how new and existing investments can be best utilized with appropriate quality expectations.

One of the problems that the industry has is that tolerances are often specified by what people find more convenient and not on what the process is capable to conform to.

In theory the price of a printed job should be a function of the variability of the ink density. Jobs printed with little variability, which translates to more precise color, should price higher relative to jobs with large variability or less precise color. Print buyers would like the most precise and most accurate color. Printers would like tolerances that permit comfortable placement of the inherent process variability. The problem is that often times, neither the printers nor the buyers know exactly what the inherent variability of the press is throughout the printing plane and between prints and they only focus on the variability of the color bars.

Therefore, a systematic look at total variability of a printing system is a prerequisite to intelligently formulating realistic tolerances.

1.2. Problem Statement

Printing uniformity is central to the wide range of standards and specifications that focus on image quality and process control. The present problem is that there is only a limited body of work independently addressing either the spatial or temporal domain of printing uniformity. There is no seminal work to reconcile various research efforts. Currently, the dominant problem is in the lack of consensus on concepts, models, and subsequently, testing methods used by contributing researchers.

The literature offers a range of works with differing and specialized objectives and motivations, but there is no common reference. Simply put, there is a wide range of parallel efforts with disparate terminologies for the same set of concepts, which entailed differences in how authors model and test uniformity. We find, for example, that for authors who explored spatial uniformity, some measured variability in printing density at ad hoc locations around the printing plane (Breede, 2007; ISO, 2007), while others used systematic repeating patterns of equally sized patches adapted to different press sizes (Sigg, 2007; Abdel Motaal & Sikander, 2009). For all intents and purposes, all methods validly measure spatial uniformity; they all quantify some aspect of evenness, but the results are difficult to compare.

Such inconsistencies occur when authors have no guiding framework and each interpret and test the same fundamental concepts differently. This problem necessitates taking steps to finding common ground for reconciliation before further experimentation in order to harmonize the contributory value of all successive research.

1.3. Purpose of the Study

This work explores the topic of printing uniformity with intent to formalize a framework of concepts and a set of device- and process-independent image quality metrics (IQMs) for benchmarking and evaluating the spatial-temporal uniformity of printing systems relative to standard industry tolerances.

1.3.1. Research Objectives

The researcher believes that the first step for understanding printing uniformity should focus on the conceptualization and modeling of this phenomenon. Subsequently, with a set of concepts and models serving as common grounds, researchers can more effectively evaluate and compare uniformity across printing systems and processes.

Three main objectives are outlined for this work:

1. Devising a set of concepts and indicators for printing uniformity.
2. Developing a set of metrics for printing uniformity.
3. Refining procedures for sampling and measuring printing uniformity.

An additional objective is also outlined for this work:

4. Devising graphic visualization techniques and data labeling schema.

A conceptual framework is defined to incorporate indicators for spatial-temporal printing uniformity through the refinement of concepts from existing works and technical documents, i.e., standards and specifications. The intended purpose of this framework is to establish practical indicators for developing quantitative models and testing methods.

Quantitative models are subsequently defined for the indicators based on common descriptive statistical measures for central tendency and variance. The intended purpose of the metrics is to quantify various aspects of uniformity (i.e. accuracy and precision) for the entire image and within regions of interests, quantifying spatial trends (i.e. evenness, directionality and proportions) and temporal trends (i.e. repeatability and reproducibility).

Various printing systems are then tested to provide sample data. The intended purpose of data is to provide usable real-world examples for refining and validate the framework and metrics. This is done by sampling density at a high spatial frequency within the printing plane between a series of prints.

The outcome of the three research components is intended to fulfill the principal purpose of offering a cohesive platform that can be used by interested researchers for theoretical study, practical testing, and, furthering the scope of quality standards.

In addition to the concepts, models, and procedures, it is also essential to devise techniques to visualize the data for analysis and reporting. This is achieved by trying different 2-dimensional and 3-demonsional plots together with various labeling schemas to capture the quantitative data in practical and informative charts.

1.4. Reasons for Interest in Topic

There are a number of reasons why this topic seems to be ideal here, including:

- Previous experience and published research on printing uniformity.
- Collaboration with one of the authors on the topic, as secondary advisor.
- Realization and resolution of fundamental limitations in previous methods.
- Availability of new press technologies to analyze and compare.
- Deeper understanding of the fundamentals, including statistics and color theory.
- Existence of previously developed analysis software further improved for this study.
- Personal conviction to challenge a common ideology that dismisses spatial uniformity as being "insignificant" or "unimportant" to printing quality due to the limitations of control on press, which stands against the very core of research work.

1.5. Definition of Terminology

This section provides definitions for terminology essential to the understanding of the underlying concepts conveyed in the reviewed literature. Definitions for the proposed framework are not included here and are thoroughly defined in *Chapter 3*.

1.5.1. Conceptual Terminology

Dimension	"A specifiable aspect of a concept" (Babbie, 2011, p. 136).
Construct	"Theoretical creation […] based on observations but that cannot be observed directly or indirectly" (Babbie, 2011, p. 133).
Indicator	"An observation that we choose to consider as a reflection of a variable we wish to study" (Babbie, 2011, p. 135).
Metric	A stipulative term used to indicate a quantitative model for a clearly defined indicator of a given attribute.

1.5.2. Statistical Terminology

Accuracy	A "comparison of a measured value with a reference value. A highly accurate measurement is one for which the difference between the measured and reference values is small whereas an inaccurate measurement is one for which the difference is large. [...] Common references in printing are the process aims defined by organizations like SNAP, GRACoL and SWOP" (Siljander & Fisch, 2001, pp. 62-63).
Precision	A measure of dispersion of sample data around the sample average. "As the number of samples increases, the precision of the average value also increases" (Siljander & Fisch, 2001, p. 62).
Standard Deviation	A measure of precision that describes "the spread of measurements about the sample average" (Siljander & Fisch, 2001, p. 62).
Standard Error	A measure of precision that describes "the spread of averages if samples are replicated" (Siljander & Fisch, 2001, p. 62).

1.5.3. Print-Related Uniformity Terminology

Printing Uniformity	Extent of the spatial and temporal uniformity, i.e. the accuracy and precision, for any attribute specific to the process of printing, i.e. the transfer of an image onto a substrate (e.g. density).
Spatial Uniformity	Extent of uniformity of a printed sheet for any given attribute (e.g. density) within the individual impression.

Temporal Uniformity	Extent of uniformity of a press or printed sheets for any given attribute (e.g. density) between a range of impressions.
Evenness	*Uniformity within sheets at frequencies visible to the viewer.*
Repeatability	Uniformity between prints from the same pressrun.
Reproducibility	Uniformity between prints across identical pressruns.
Stability	Degree of post-printing curing of materials, or the timeframe of.
Durability	Degree of functional resilience against wear, or the timeframe of.

1.5.4. Print-Related Technical Terminology

Printing Density	Stipulative term inexplicitly describing the extent of light absorption rendered onto reflective media for image reproduction, which may refer to optical density or other measures of intensity.
Optical Density	Negative logarithm to the base ten of the reflectance factor, measured using a 0/45-degree geometry, Illuminant A, and ISO visual density calibration as specified in ISO 5-1, 5-3 and 5-4 with an instrument using no polarization filters (ISO, 2012, p. 3).

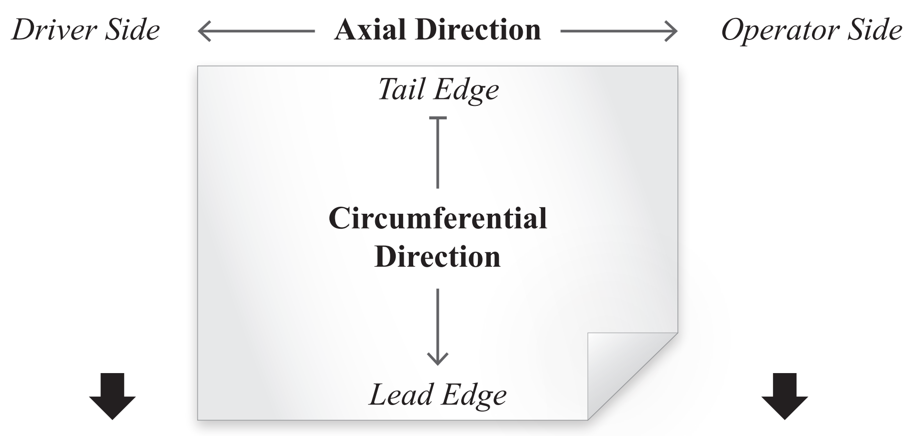

Figure 2. Dimensions of a printing press as they related to the printed sheet.

Edge,	*Lead*	Press sheet edge leading through at the printing nip, see *Figure 2*.
	Tail	Press sheet edge trailing behind at the printing nip, see *Figure 2*.
Side,	*Driver*	Side of press where gears are located; aka gear side, see *Figure 2*.
	Operator	Side of press where operator controls are located, see *Figure 2*.
Direction,	*Axial*	Parallel to the axis of the impression cylinder, see *Figure 2*.
	Circumferential	Perpendicular to the axis of the impression cylinder, see *Figure 2*.

Chapter 2
Literature Review

This chapter provides a synopsis of reviewed literature addressing immediate and peripheral aspects relating to the conceptual framework, quantitative models and test method.

2.1. Overview of the Selected Literature

A number of authors have published works examining immediate and peripheral aspects of printing uniformity. This review identifies the various contributions in the different aspects of the topic but focuses mainly on research that is immediately related to the topic and the three exploratory objectives. Several technical documents were also referenced and are central to this work, which were selected from popular industry references where uniformity ought to be addressed.

2.2. Research Works

The first related work identified was regarding the ‘Accuracy and Precision in Color Characterization’ by Siljander and Fisch (2001). It offers statistical means for analyzing the uniformity within prints in an effort to improve standard practices for press characterization. The second one was on the ‘Spatial Uniformity of Offset Printing’ by Sigg (2007). It examined the uniformity of inking in the spatial domain. The third was on ‘The Effect of Ink Film Thickness Variations on Color Control in the Circumferential Printing Cylinder Direction of Offset Presses’ by Breede (2007). It explored the directionality of spatial variability. The fourth was on the ‘Repeatability of Ink Transfer and Color Management in Lithography’ by Abdel Motaal and Sikander (2009). It examined spatial and temporal uniformity aspects for two lithography presses. Comparisons of specific aspects are presented in following sections.

2.2.1. Technical Documents

Some ISO technical standards on ‘Graphic Technology’ are essential to the topic including: a) ISO 12637-3 (2009) which covers pertinent printing terminology; b) ISO 12647-2 (2004; 2007) which cover process control standards for offset lithography; and, c) ISO/CD 15311-1 (2011) which “provides a framework of image and product quality criteria” including parameters and measurement methods related to large format digital printing. Also of importance is ISO/TS 24790 (2012) on ‘Measurement of image quality attributes for hardcopy output’ pertaining to single-color prints using office equipment.

2.3. Concepts

Printing uniformity is a subset of the broader topic of imaging uniformity. It is the extent to which the actual printing density is uniform, i.e. both accurate and precise, throughout the each printed sheet (spatially) and between sheets (temporally).

2.3.1. Accuracy and Precision

Siljander and Fisch (2001) describe a statistical approach to determine accuracy and precision of printing, illustrated in *Figure 3*. Accuracy is determined relative to a reference value based on the sample and population averages. Precision for a set of samples is quantified using the control limits, which factor in the standard deviation.

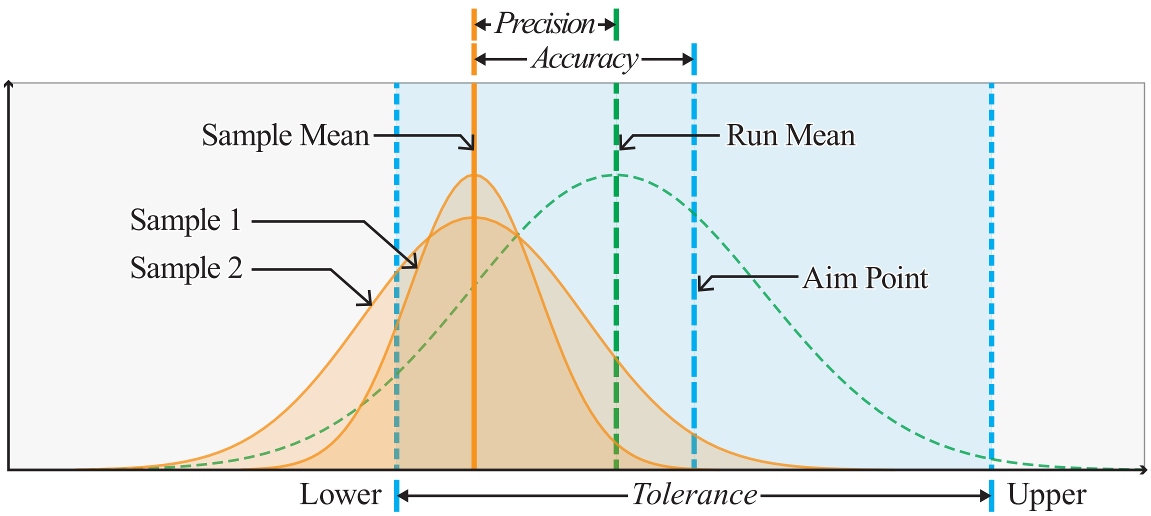

Figure 3. Accuracy and precision as illustrated by Siljander and Fisch.[1]

From this work, it can be assumed that accuracy and precision are two statistical dimensions that can be used to quantify uniformity. This means that a system can be considered uniform when it is both accurate and precise, which is the natural ideal state of a system. Accuracy and precision are subject to degradation due to systematic and random causes. This leads to the inaccuracy and imprecision constructs defined below.

Inaccuracy. Deviation, referred to by this author as inaccuracy, is defined as one of the conformance criteria for the process-color in ISO 12647-2 (2004, p. 6) and tone-value increase (2004, p. 12), which affects “color difference between proof and OK prints”.

Imprecision. Variation, referred to by this author as imprecision, is defined as one of the conformance criteria for the process-color in ISO 12647-2 (2004, p. 6) and tone-value increase (2004, p. 12), which affects color variability in a representative sample for a run.

[1] Adapted from Siljander & Fisch (2001), *TAGA Proceedings*, (p. 57-78).

2.3.2. Spatial Domain

Figure 4 illustrates a number of concepts or dimensions that are contained within the spatial domain in the realm of printing with reference to sheet alignment and scale.

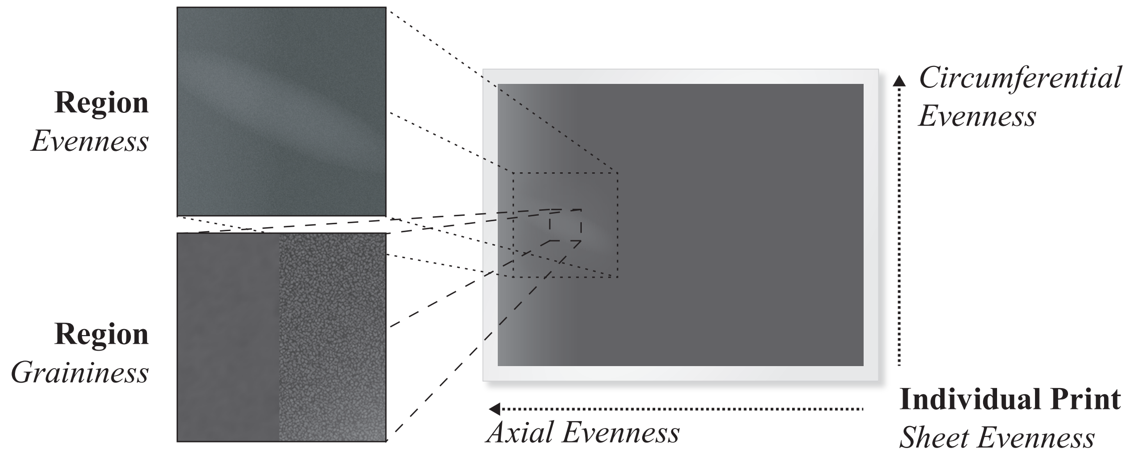

Figure 4. The spatial domain relative to spatial frequency and sheet alignment.

Spatial Dimensions. Authors have made distinctions between the two spatial dimensions of the printing plane relative to the print direction.

The dimension parallel to the print direction is consistently referred to as the circumferential dimension (Breede, 2007; ISO, 2009, p. 3; Abdel Motaal & Sikander, 2009). The dimension perpendicular to the print direction is referred to as the axial or lateral dimension (Breede, 2007; Ploumidis , 2007; Abdel Motaal & Sikander, 2009).

Spatial Evenness. Evenness has used to describe uniformity in “solid printed areas” (Eerola, et al., 2010, p. 2; Seymour, 2008, p. 218) and ink film thickness (Seymour, 2008, p. 218; Breede, 2007, p. 70).

Evenness was paired with terms describing directionality, i.e. circumferential and lateral, and spatial divisions, e.g. ink zones (Sigg, 2007; ISO, 2007; Abdel Motaal & Sikander, 2009).

2.3.3. Temporal Domain

Figure 5 illustrates a number of concepts or dimensions that are contained within the temporal domain in the realm of printing for different reference points or contexts.

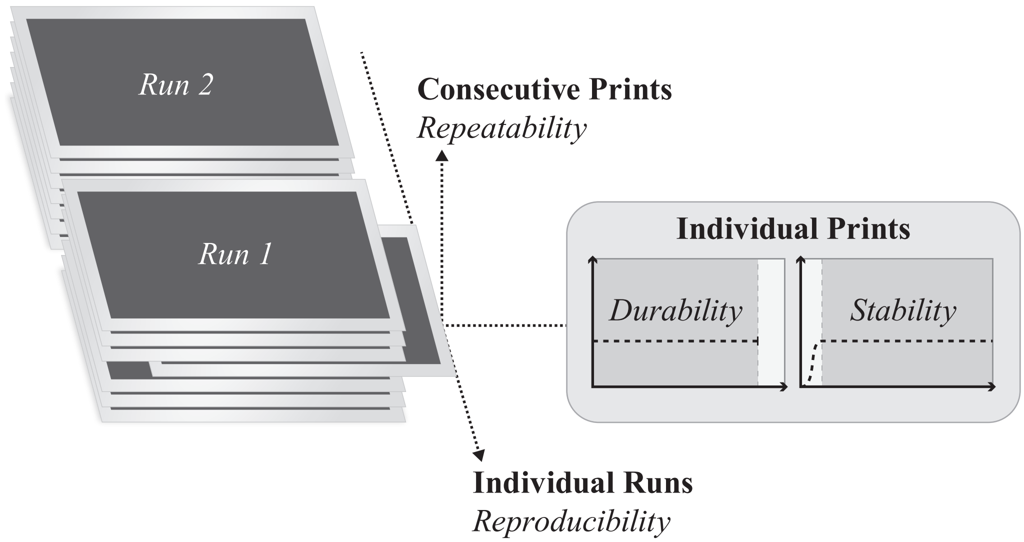

Figure 5. The temporal domain relative to prints and pressruns.

Temporal Dimensions. Authors have distinguished between various temporal dimensions in printing for individual impressions and between impressions.

Individual impression dimensions relate to the lifespan of a printed image inferred from definitions like print stabilization period "till a stable color is achieved" (ISO 12647-7:2007). Between impressions dimensions fundamentally include sheet-to-sheet (or between-sheets) and run-to-run (or between-runs), not excluding additional contexts.

Temporal Repeatability and Reproducibility. Repeatability and reproducibility have been been used in the printing realm to respectively indicate variability between prints and runs, not to mention the various uses within the realm of statistics and metrology (Seymour, 2008; Radencic, Neumann, & Bohan, 2008).

A distinction was made in the CGATS recommended practices for "Procedures for color measurement system process control and inter-lab coordination" (2007, p. 2) in which repeatability was associated with measurements taken after one another within a short time under the same condition, whereas reproducibility was associated with those taken under different conditions.

2.4. Quantitative Model

2.4.1. Metrology

Various authors on the topic of printing uniformity used density as a key measure for the extent of variability. Authors have also employed colorimetric measures such as Delta-E (Abdel Motaal & Sikander, 2009; Breede, 2007; Sigg, 2007). Colorimetric measures were used mostly in conjunction with density to signify the extent of perceived color difference associated with observed variability in density.

Density has been the standard industry measure for the ink film thickness from the mid of the 20th century until 2004 when it was formally replaced with colorimetry in primary international standards and subsequent specifications (ISO 12647-2:2004). Densitometers were central to print process control as they made it possible to define and enforce aim points and tolerances based on objective measures of the ink volume (Seymour, 2008).

Formal adoption of CIELAB occurred in more recent revisions of various standards and specifications (ISO 12647-2:2004; GRACoL-7:2007). This transition is gradually replacing the use of densitometry for process control applications. However, colorimetry is not new to the realm of printing. Aside from the specific uses for process control in the pressroom, it has long been used by the industry. *Figure 6* shows the CIELAB color space and the CIExyY chromaticity diagram for the CIEXYZ color space using a transformation for the chromatic components X and Z.

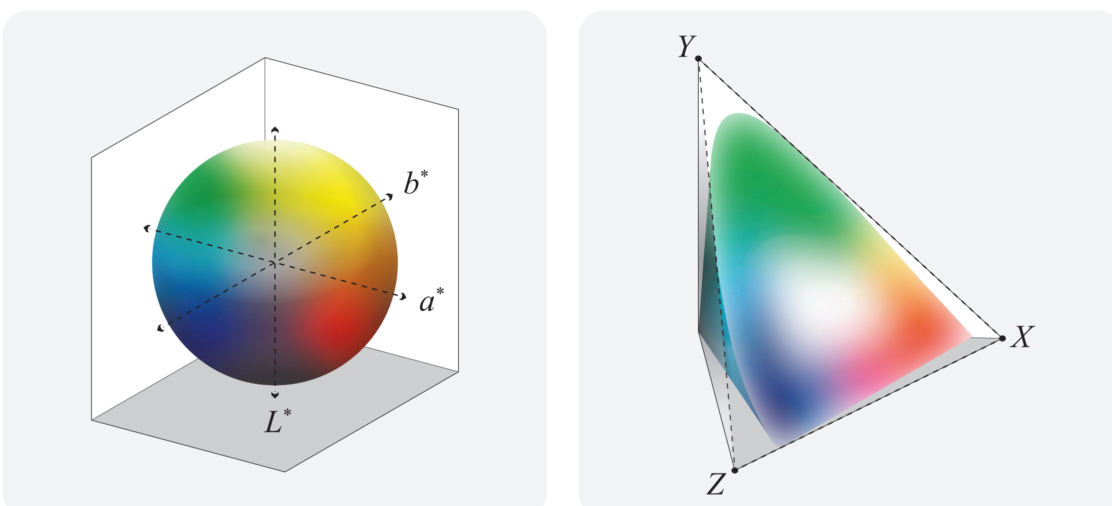

Figure 6. CIELAB and CIEXYZ color spaces.[2]

[2] CIE-XYZ plot adapted from http://en.wikipedia.org/wiki/Color_model
CIE-LAB plot adapted from

Key differences between the sensitivities of density and CIELAB make each one more suitable for specific applications. CIELAB is suitable for perceptual color assessment and quantification of perceived color difference. On the other hand, density was deemed more suitable for measuring uniformity for the following two advantages.

The first advantage is the fact that density uses logarithmic scaling which makes it more sensitive to variations in darker colors, as illustrated in *Figure 7.* Higher sensitivity in the dark region makes it practical when fine-tuning the flow of ink on the press, which makes it also practical to use when measuring printing uniformity.

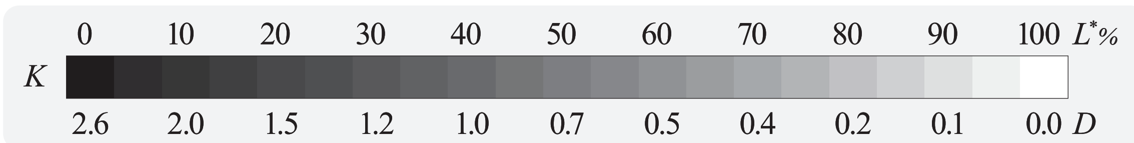

Figure 7. Comparing the CIE-L* and Visual Density lightness scales.

The second advantage to density is that it uses filters for the different colors, cyan, magenta, yellow and black to measure the intensity of the received light particular to the respective inks. *Figure 8* illustrates how a densitometer uses filters for the different inks.

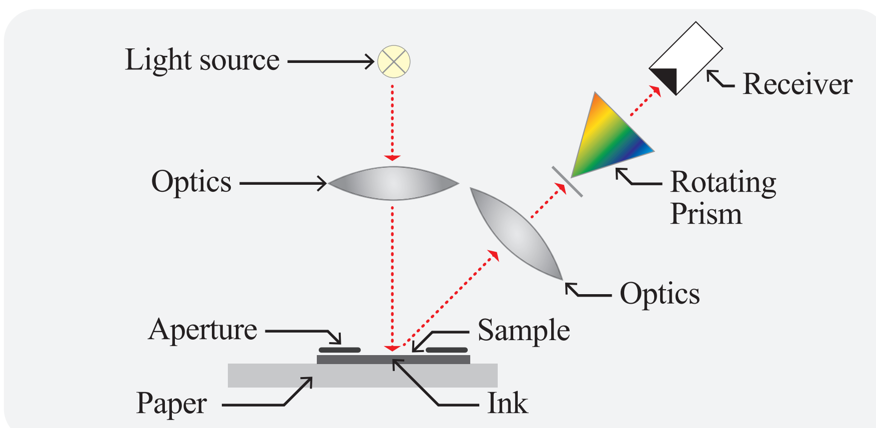

Figure 8. Conceptual diagram of a densitometer using color-specific filters.[3]

Colorimeters also use filters, but unlike densitometers they use filters that are can emulate human perception, not chromatic filters. However, there are no mathematically derived colorimetric components that can offer similar functionality for each ink. For instance, CIE-L* may work well for black ink but it does not function the same for the other primary colors. As such, density seems to be the better choice since it offers a single measure adaptable to different inks using respective filters or mathematical functions.

[3] Adapted from Kipphan, H. (2001), *Handbook of Print Media* (p. 101).

2.4.2. Metrics

Siljander and Fisch's Accuracy and Precision. In their work, accuracy was determined relative to a reference value based on the sample and population averages. Precision for a set of samples is quantified using the upper and lower control limits determined by the standard deviation. *Figure 3* is shown once again below to illustrate those concepts.

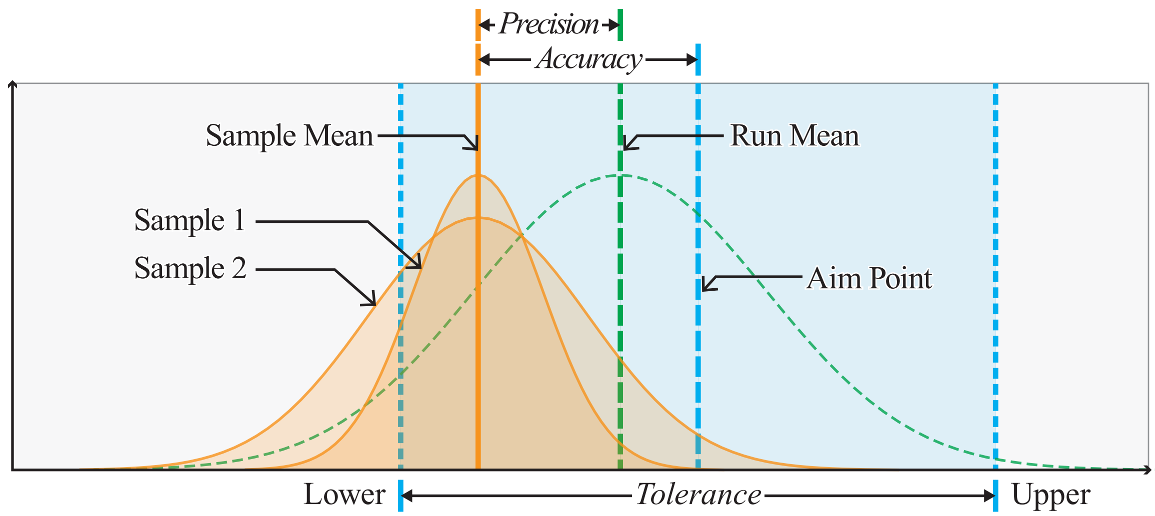

Figure 3. Accuracy and precision as illustrated by Siljander and Fisch. (repeated, pp. 20).

A number of statistical terms were described in detail by the authors, including: a) sample size; b) sample average; c) population average; d) sample standard deviation; e) population standard deviation; and, e) standard error. The reader is referred to the Definition of Terminology for definitions for some of the above terms.

Rech's Degree of Unevenness. The degree of unevenness (*Equation 26*) is calculated based on the range between the lightest and darkest values sampled relative to the mean of all the samples (Breede, 2007). Rech's formula is very similar to one used in some studies in the realm of medical imaging involving the analysis of the image volume uniformity for 3D PET (positron emission tomography) systems (Oakes, Sossi, & Ruth, 1997). The degree of unevenness was considered "the most important quality index" since it factors in the extremes of the ink film thickness (Breede, 2007; Rech, 2010).

Breede (2007) demonstrates the application of the degree of unevenness in analyzing ink film thickness variations. He applied this formula to 10 measurements sampled along circumferential solid color strips for all four channels (CMYK). The analysis compared the degree of unevenness of an office-class electrophotographic printer and a direct imaging offset lithographic press. The most crucial outcome noted was that both systems exhibited, almost equally, a substantially large degree of unevenness relative to the 3% aim point adopted from the original author's work.

M-Score. Fogra (Kraushaar, 2013) developed M-Score to look at the extent of variability based on the CIE ΔE00 color difference between neighboring patches using a special test target. M-Score is designed to provide a measure of evenness that improves upon the standard "9-point method" for testing the evenness of proofers (ISO 12647-7:2007).

M-Score provides a single number that is more specialized than variance and standard deviation to printing uniformity applications, namely spatial evenness. While the single number aspect is suited for benchmarking and comparing systems and processes, it is also a limitation to how this metric can be applied in the study. M-Score does not factor in the temporal dimension and this is important for the present work. Furthermore, omitting the spatial coordinates in favor of a single number takes away the ability to capture the patterns of unevenness.

Ultimately, M-Score can be used to provide another measure for imprecision if it were measured separately across distributed regions and between several impressions. However, this is beyond the scope of this work.

ISO Graininess and Mottle. Graininess and mottle (ISO/TS 24790:2012), which measure evenness at different spatial frequencies were also reviewed. Although they apply to scanned images with much higher spatial sampling, they offered great insights and added merit to some of the metrics proposed in this work.

Those metrics operate on the principle of using the weighted sum of the squared standard deviation, which is used in the proposed models to deal with the complexities of the various spatial and temporal dimensions.

2.5. Testing Methods

The reviewed works had significantly different testing methods. Aside from the fact that all authors tested one or more presses including lithography presses, the procedures were very unique, hence the reconciliation efforts applied in this work.

Breede (2007) tested one offset press and an office-grade four-color laser printer. Both jobs were made from the same digital file, or, in other words, the same test forme was used in both tests.

The first test compared a single sheet from each run, which was used to confirm the existence of circumferential variability. The second test compared three offset prints with “progressively decreasing amounts of ink” to observe changes in the circumferential variability pattern and to gauge the extent of perceived color shift.

Siljander and Fisch (2001) conducted tests on at least three different offset presses. The focus here was to compare the “within sheet” and “between sheet” variability for actual “press tests intended to meet SWOP specifications” as well as the consistency between the measured variability at the color bar versus the entire sheet.

Sigg (2007) conducted tests on a single offset press and a high-end industry-grade multicolor dye-sublimation proofer. Ink film thickness variability was observed in a previous unrelated study, which prompted this work.

Systematic elimination was used to explore the effect of prepress and pressroom variables on observed variability, or ‘wiggles’. From these pretests, spatial ink film thickness variability was deductively attributed to on-press factors.

Abdel Motaal and Sikander (2009) tested two offset presses, including a multicolor unit-configuration landscape press and a multicolor satellite-configuration direct imaging portrait press. The focus was on comparing spatial and temporal variability of the presses against ISO 12647’s CIELAB and historical density thresholds.

The runs were conducted using different test formes optimized for the different formats, which were measured using an automated sheet-fed spectrophotometer.

2.5.1. Spatial Sampling

On the spatial domain, the sampling differed substantially between all four works. These differences proved valuable in the determination of the spatial sampling that was adopted for this work, which seeks to build on the lessons learned from past efforts.

Breede (2007) collected ten samples along the length of both axial and circumferential solid ink strips, as well as patches with 10-step tone increments for the primary and secondary colors that were oriented circumferentially.

Siljander and Fisch (2001) collected samples from replications of randomized IT8 target printed on each sheet; those targets contain patches for the primary and secondary solids as well as a variety of tones. It should be noted that Siljander and Fisch used multiple measurements within sheets as means for increasing statistical certainty.

Sigg (2007) first sampled replications of RIT 100 Randomized Steps Chart similar to the IT8 used by Siljander and Fisch. Sigg followed by sampling 266 uniformly spaced replicates for solid and mid-tone primary colors. The higher spatial resolution made it possible to construct a three-dimensional spatial uniformity profile, in *Figure 9*. The profile offers valuable insights on spatial unevenness, which is essential to this study.

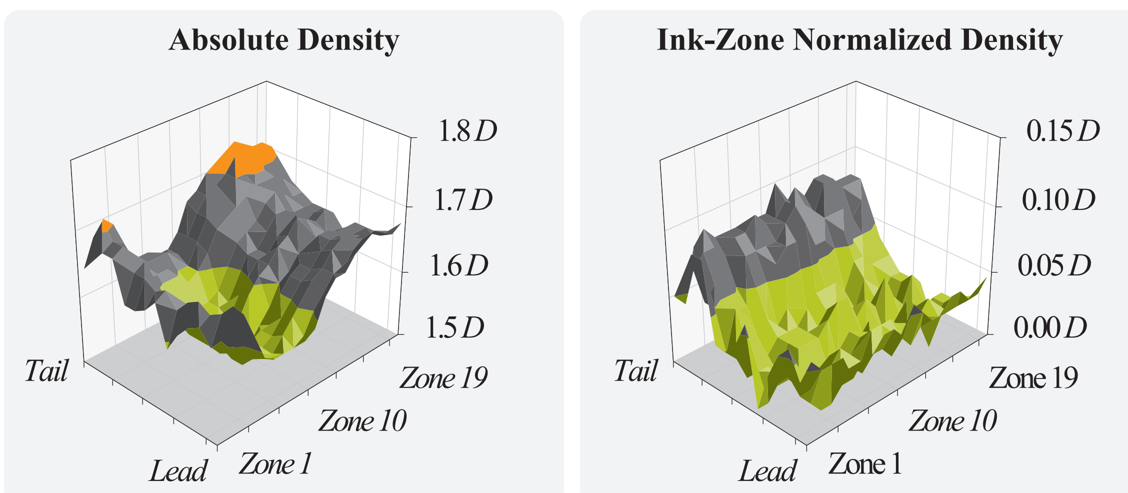

Figure 9. Sigg evenness profile for magenta using 266 data points[4].

Abdel Motaal and Sikander collected samples from multiple replications of the basic IT8 that is limited to 96 patches thus allowing for 9 and18 repeats on the smaller and larger presses, respectively.

[4] Adapted from Sigg, F. (2007). *TAGA Proceedings*, (p. 649-658).

2.5.2. Temporal Sampling

On the temporal domain, the reviewed works did not provide much insight as some have only focused on spatial uniformity. Breede (2007) and Sigg (2007) have limited their analysis to a single press sheet. Siljander and Fisch (2001) took a number of samples, around 8 prints, for the portions where they analyzed the "between sheets" as well as for statistical determination of the accuracy and precision. Abdel Motaal and Sikander (2009) examined 11 prints taken from a set of 100 consecutive prints, including the first and last prints, and nine prints taken at random, one every ten consecutive prints.

Due to the differences across the previous work, it is essential to look for references that provide proven strategies for sample selection. Strategies that were identified would be integrated together to devise a final strategy for use in this work. These strategies were chosen from the CGATS 'Color Characterization Data Set Development' documents and are discussed below. CGATS outlined strategies for sampling in their 'Press Run Guidelines' (2003) and 'Analysis and Reporting' (2007) documents, which must be considered at this point. The three strategies considered include random, uniform, and sequential sampling, each of which would be suited in different scenarios depending on the available knowledge of sources of the variability.

Random Sampling. Samples are selected using a random number generator:

> "Random sampling is suggested in cases where the printing conditions are believed to be consistent and stable within the press run and no particular efforts are [were] made to tune a specific portion of the press run. The use of random samples also allows other statistics about printing variability within the specific press test to be developed." (CGATS Analysis and Reporting Guidelines, 2007; p. 2)

Uniform Sampling. Samples are pulled at a steady interval or a set time duration:

> "Uniform sampling addresses long term drift in printing conditions within a press run. It is typically taken from a press run at uniform intervals. The uniform sampling method is suggested in cases where the long term variation of the press is deemed unacceptably large." (CGATS Analysis and Reporting Guidelines, 2007; p. 2)

Sequential Sampling. Samples are pulled in order from the stack:

> "Sequential sampling addresses sheet-to-sheet variation [...] Sequential sampling is suggested in cases where it is felt to be important to apply specific controls or adjustment of printing conditions, within a press run, to ensure a close match to the specified aims and tolerances." (CGATS Analysis and Reporting Guidelines, 2007; p. 2)

2.6. Conclusions

The terminology used throughout the literature indicates conceptual agreement on the characterization constructs of printing uniformity. However, the terms used have varied between the authors, and more importantly, are in some cases not formally and clearly defined in standards and specifications.

There is a need for formal definitions regarding the dimensions of printing that would agree with popular and rather instinctual inferences made by various authors. These definitions should recognize the within sheet, within spatial regions of interest, between sheets, runs, and over time dimensions in the spatial and temporal domains.

Previous works have used both density and colorimetry as a measure of the ink variation and color difference. However, the same considerations do not apply to this study since we are restricted to a single color, namely black. It is concluded that the different measures must be compared in order to select the measure that would be ideal.

Both accuracy and precision are fundamental to the quantification of printing uniformity. The reviewed literature includes various calculation methods, which ought to be explored. This work should develop a metric based on the work of Siljander and Fisch.

The degree of unevenness, by Rech, shared resemblance to measures used outside the realm of print. This work should incorporate Rech's approach in devised metrics.

For spatial sampling, Sigg's design must be considered in this work due to its high resolution. For temporal sampling, CGATS outlined random, uniform, and sequential sampling strategies that must be considered at this point.

Chapter 3
Conceptual Framework

This chapter introduces the conceptual framework developed and proposed in this study. The framework defines clear dimensions, constructs, and, indicators for process-independent evaluation of printing uniformity. These concepts are refined through reconciliation of the literature in *Chapter 2*. The framework concludes with a set of indicators that lay foundations for the models in *Chapter 4* and methods in *Chapter 5*.

3.1. Introduction

This framework deals with a number of concepts that relate to the extent of uniformity across spatial and temporal domains. The framework incorporates dimensions, constructs and indicators in a hierarchical structure for conceptualization.

Dimensions define a scope for conceptualizing phenomena. For instance, printing accuracy and precision dimensions set the scope for conceptualizing printing uniformity.

Constructs are theoretical conceptions that reflect some quality or attribute relating to a given phenomenon. For instance, regional accuracy is a construct that refers to the extent of accuracy in a given region of interest. Regional accuracy is intuitively conceivable from the two broader concepts 'regions' and 'accuracy'. Constructs are abstract conceptions. They are not concrete, and, as such, not measurable.

Indicators are operational definitions that are both concrete and measurable, which bridge abstract constructs to concrete representations. For example, it is possible to define an indicator like 'regional inaccuracy score' in order to provide concrete indication regard the extent accuracy within regions, provided there is a concerete measurable aspect.

3.1.1. Scope and Limitations

This work focuses on printing accuracy and precision, which are key dimensions of variability in the field of statistics. The framework introduces constructs and indicators that reflect the extent of accuracy and precision within given spatial-temporal frames. It features a basic set of device- and process-independent constructs and indicators for statistically describing and qualifying the uniformity of the printed image as a function of the expected spatial and temporal variance in the actual versus intended density.

The framework does not address process- and device-specific characteristics nor does it address cause-effect relationships, notwithstanding their significance and relevance in many applications. Statistical indicators state with a degree of certainty a probability for variability, but they don't predict variability at a given moment or place.

3.2. Printing Uniformity Framework

The Printing Uniformity Framework is a conceptual framework that deals with the evaluation and benchmarking of the uniformity of printing systems across different system, press designs and printing processes. The framework lays foundations for the development of a quantitative metric for the measurement and characterization of the uniformity of printing systems through a set of generic output-centric indicators.

3.2.1. Conceptual Order

In order to conceive the uniformity of a given printing system it must be possible to conceive both the accuracy and precision dimensions specifically.

The terms printing accuracy and printing precision are used to convey the two dimensions. Each dimension encompasses a set of constructs and indicators as shown in *Figure 10*. The dimension can be conceived through the set of constructs, which can be inductively conceived through the set of indicators.

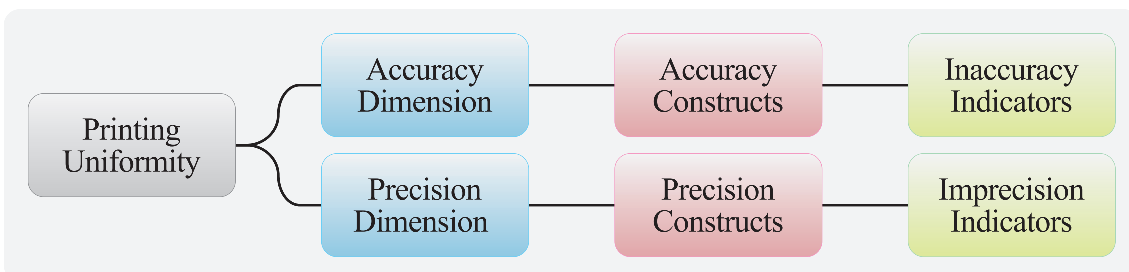

Figure 10. Printing uniformity dimensions, constructs and indicators overview.

3.2.2. Printing Uniformity Dimensions

Figure 11 shows the dimensions of the framework defined below.

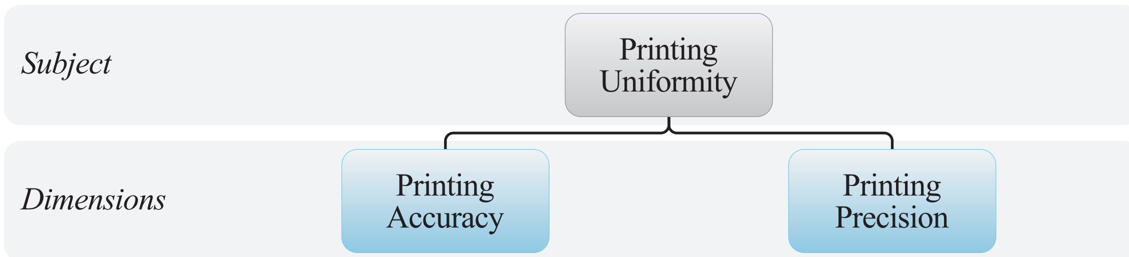

Figure 11. Printing accuracy and precision dimensions.

Printing Accuracy. The printing accuracy dimension reflects the extent of uniformity attributed to shift in central tendency for a sample relative to intended density.

Printing Precision. The printing precision dimension reflects the extent of uniformity attributed to the dispersion for a sample.

The curves in *Figure 12* are adapted from Siljander & Fisch to illustrate how each dimension relates to the entire run, sheets, bands, regions and patches.

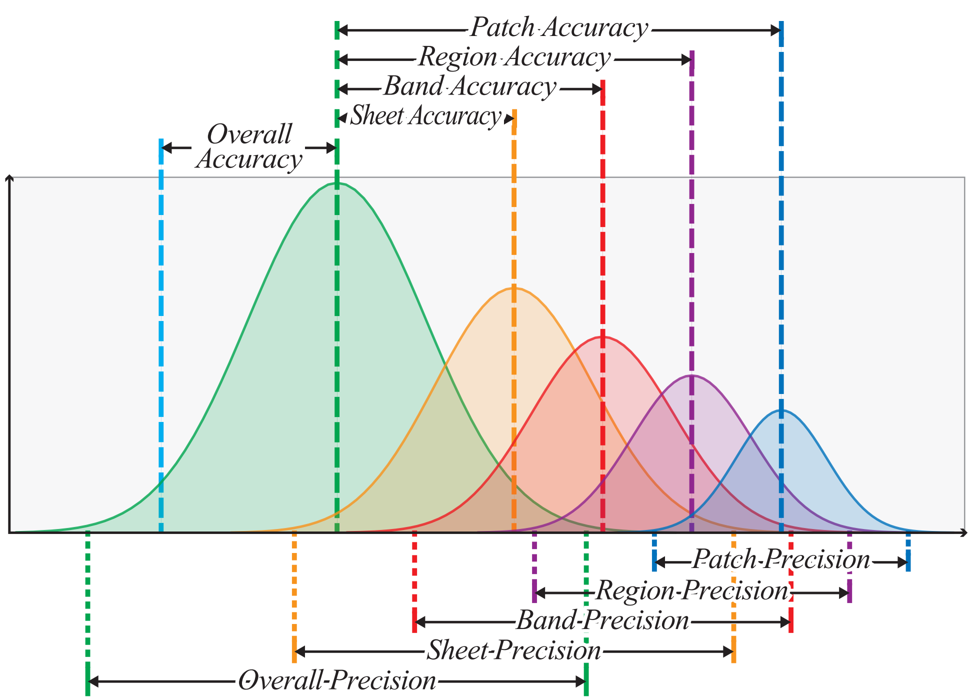

Figure 12. Visualization of printing accuracy and precision.

3.2.3. Printing Uniformity Constructs

Figure 13 shows the constructs of the framework defined below.

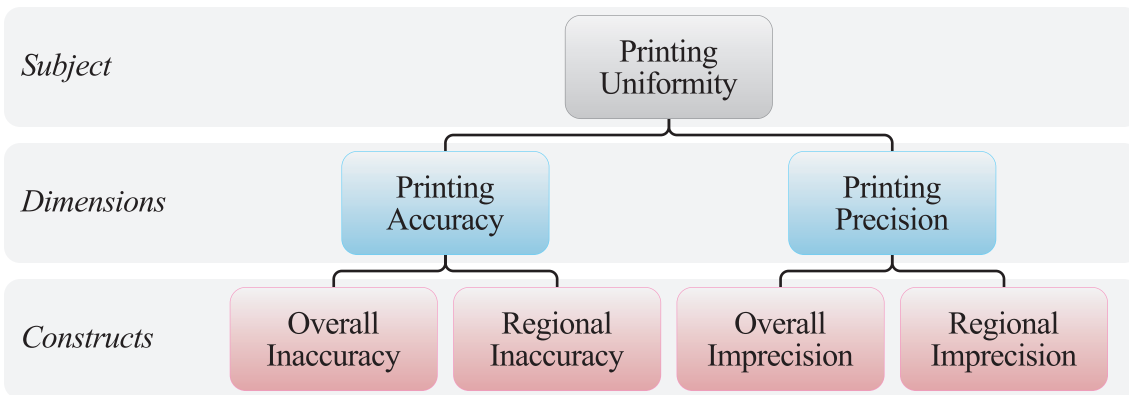

Figure 13. Printing accuracy and precision constructs.

The fundamental distinction between the overall uniformity of a pressrun and that of a particular spatial subset or region of interest entails the need for separate constructs.

Overall Accuracy & Precision. The uniformity of an entire pressrun is a function of the accuracy and precision throughout the spatial and temporal domains. Overall accuracy reflects the accuracy of the entire run, which is defined by the central tendency across the domains relative to a standard aim point. Overall precision reflects the precision of the entire run, which is defined by the dispersion across the domains.

Regional Accuracy & Precision. The printing uniformity of any region of interest is a function of the accuracy and precision within the spatial region or band subset and throughout the temporal domain, illustrated in *Figure 14*. Regional accuracy is defined by the central tendency across the subset relative to the entire run. Regional precision is defined by the dispersion across the subset. Regional accuracy is different from run accuracy in that it references the mean for the run instead of a predefined aim point.

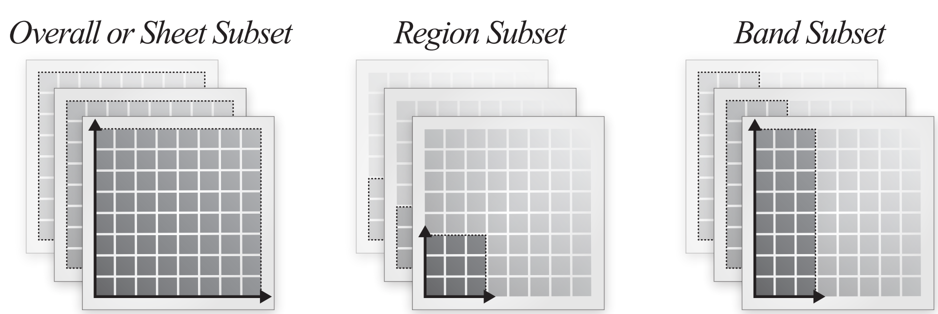

Figure 14. Overall versus sheet, region, and, band spatial subsets.

3.2.4. Printing Uniformity Indicators

Figure 15 shows the indicators of the framework defined below.

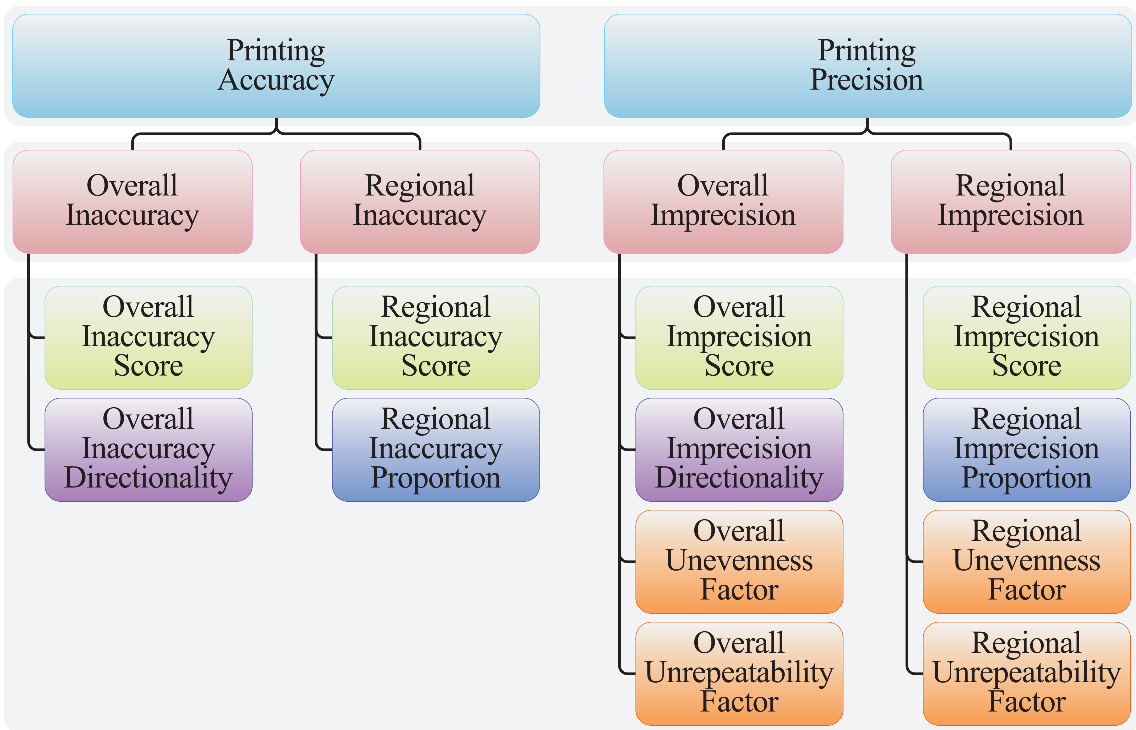

Figure 15. Printing accuracy and precision dimensions, constructs and indicators.

Inaccuracy Scores. Overall and region inaccuracy values are compared against one-half of the standard tolerance for printing density to determine scores for each.

Inaccuracy Directionality. Variance between band inaccuracy values in either the circumferential or axial dimensions determine overall directionality for each dimension.

Inaccuracy Proportions. Regional inaccuracy values are compared against the sum of all the regional inaccuracy values for any given subset, including bands and regions.

Imprecision Scores. Overall and region imprecision values are compared against the standard tolerance for printing density to determine scores for each.

Imprecision Directionality. Variance between band imprecision values in either the circumferential or axial dimensions determine overall directionality for each dimension.

Imprecision Proportions. Regional imprecision values are compared against the sum of all the regional values for any given subset, including bands and regions.

Imprecision Factors. Variance for the spatial or temporal domains are computed for each sheet or patch respectively to determine the unevenness and unrepeatability factors.

Chapter 4
Quantitative Models

This chapter introduces the quantitative models developed and proposed in this study. The quantitative models are devised for all indicators in *Chapter 3*. These metrics are also based on the literature, which was reviewed in *Chapter 2*. Predefined color and statistics models are introduced at the end.

4.1. Printing Uniformity Models

Models for the printing accuracy and precision dimensions, as defined in section *3.2.2*, are devised for overall (generalized) and regional (localized) constructs. They are defined in section *3.2.3*, for each of the indicators, which in turn are defined in section *3.2.4*.

4.1.1. Metrics for Run and Regional Constructs

Run Metrics. Metrics that reflect the extent of uniformity for all the patches of an intended tone value across all the prints. They are based on sample criteria defined in the testing methods, and include scores and circumferential or axial directionalities.

Regional Metrics. Metrics that reflect the extent of uniformity for all the patches of an intended tone value across all the prints within a specific region of interest. They are based on the regioning strategies (regions and bands) in the testing methods, and include scores and regional proportions and spatial or temporal factors.

4.1.2. Metrics for Accuracy and Precision Dimensions

Inaccuracy Metrics. Metrics that reflect the extent of uniformity attributed to shift in central tendency for a sample relative to intended printing density, i.e. printing accuracy, include run and regional inaccuracy scores, regional inaccuracy proportions, and, circumferential or axial inaccuracy directionalities.

Imprecision Metrics. Metrics that reflect the extent of uniformity attributed to the dispersion for a sample, i.e. printing precision, include run and regional imprecision scores, regional imprecision proportions, circumferential or axial imprecision directionalities, and, spatial or temporal factors.

4.1.3. Inaccuracy & Imprecision Values

Overall Inaccuracy Value. Overall inaccuracy value is determined by subtracting the standard aim point for the intended tone value from the mean for all the patches of that tone value across all the prints, based on sample criteria defined in the testing methods.

$$v\Delta = \left(\frac{1}{N}\times\sum_{i=1}^{N} Z_i\right) - \dot{Z} \qquad \{Z_i \in Z\} \qquad \textbf{(1)}$$

Regional Inaccuracy Value. Regional inaccuracy value is determined by subtracting the mean for all the patches of the intended tone value across all the prints from the mean for all the patches of that tone value within the region of interest across all prints, based on sample criteria defined in the testing methods.

$$v\delta_p = \left(\frac{1}{n}\times\sum_{i=1}^{n} z_i\right) - \overline{z} \qquad \left\{z_i \in Z_{(p,S)} \subset Z; p \subset P\right\} \qquad \textbf{(2)}$$

Overall Imprecision Value. Overall imprecision value is determined by the sample standard deviation for all the patches of that tone value across all the prints, based on sample criteria defined in the testing methods.

$$v\mathrm{K} = \sqrt{\frac{1}{N-1}\sum_{i=1}^{N}\left(Z_i - \overline{Z}\right)^2} \qquad \{Z_i \in Z\} \qquad \textbf{(3)}$$

Regional Imprecision Value. Regional imprecision value is determined by the sample standard deviation for all the patches of that tone value within the region of interest across all prints, based on sample criteria defined in the testing methods.

$$v\kappa_p = \sqrt{\frac{1}{n-1}\sum_{i=1}^{n}\left(z_i - \overline{z}\right)^2} \qquad \left\{z_i \in Z_{(p,S)} \subset Z; p \subset P\right\} \qquad \textbf{(4)}$$

where

- $\overline{Z}$ mean density value for patches in P in all sheets
- $\overline{z}$ mean density value for patches in p in all sheets
- $\dot{Z}$ standard density value (predefined aim point)

and

- S set of all sheets in a run
- P set of all patches in a sheet
- p spatial subset of patches from P
- Z density values for patches in P (entire sheet) in all sheets
- z density values for patches in p (spatial subset) in all sheets
- N number of patches in P (entire sheet) in all sheets
- n number of patches in p (spatial subset) in all sheets

4.1.4. Inaccuracy & Imprecision Scores

Overall Inaccuracy Score. Overall inaccuracy score is determined by dividing the overall inaccuracy value by one-half the tolerance, i.e. 0.05 D for tolerance 0.10 D (±0.05 D).

$$\Delta = \left| \frac{v\Delta}{\frac{1}{2} \times \hat{Z}} \right| \qquad \textbf{(5)}$$

Regional Inaccuracy Score. Regional inaccuracy score is determined by dividing the regional inaccuracy value by half the tolerance, i.e. 0.05 D for tolerance 0.10 D (±0.05 D).

$$\delta_p = \left| \frac{v\delta_p}{\frac{1}{2} \times \hat{Z}} \right| \qquad \{p \subset P\} \qquad \textbf{(6)}$$

Overall Imprecision Score. Overall imprecision score is determined by multiplying the overall imprecision value by 6 then dividing by the tolerance, i.e. 0.10 D (±0.05 D).

$$\mathrm{K} = \frac{6 \times v\mathrm{K}}{\hat{Z}} \qquad \textbf{(7)}$$

Regional Imprecision Score. Regional imprecision score is determined by multiplying the regional imprecision value by 6 then dividing by the tolerance, i.e. 0.10 D (±0.05 D).

$$\kappa_p = \frac{6 \times v\kappa_p}{\hat{Z}} \qquad \{p \subset P\} \qquad \textbf{(8)}$$

where

$v\Delta$ overall inaccuracy value

$v\mathrm{K}$ overall imprecision value

$v\delta_p$ regional inaccuracy value for a subset of patches *p*

$v\kappa_p$ regional imprecision value for a subset of patches *p*

$\hat{Z}$ standard density tolerance (predefined tolerance)

and

p spatial subset of patches from *P*

4.1.5. Inaccuracy & Imprecision Proportions

Regional Inaccuracy Proportions. Regional inaccuracy proportions are determined by dividing the absolute values of each regional inaccuracy value by the sum of the absolute value of all regional inaccuracy values.

$$p\delta_x = \left| \frac{v\delta_x}{\sum_{r=1}^{n_r} |v\delta_r|} \right| \qquad \{x \in p_x \subset P, r \in p_r \subset P\} \qquad \textbf{(9)}$$

Regional Imprecision Proportions. Regional imprecision proportions are determined by dividing the sum of the squares of each regional inaccuracy proprotions by the sum of the squares of all regional inaccuracy values.

$$p\kappa_x = \frac{v\kappa_x^2}{\sum_{r=1}^{n_r} v\kappa_r^2} \qquad \{x \in p_x \subset P, r \in p_r \subset P\} \qquad \textbf{(10)}$$

where

- $v\Delta$ overall inaccuracy value
- $v\mathrm{K}$ overall imprecision value
- $v\delta_p$ regional inaccuracy value for a subset of patches p
- $v\kappa_p$ regional imprecision value for a subset of patches p

and

- p spatial subset of patches from P
- p_x subset of p in the region or band of interest
- p_r subset of p in the set of mutual regions or bands

4.1.6. Imprecision Factors

Unevenness and Unrepeatability Value. Overall and regional values are determined by the mean of the squares of the imprecision values for sheets or patches, for unevenness or unrepeatability, respectively.

$$v\mathrm{E} = \sqrt{\frac{1}{N_S}\sum_{j=1}^{N_S} v\kappa_{(P,j)}^2} \qquad \{j \in S\} \qquad \textbf{(11)}$$

$$v\mathrm{T} = \sqrt{\frac{1}{N_P}\sum_{i=1}^{N_P} v\kappa_{(i,S)}^2} \qquad \{i \in P\} \qquad \textbf{(12)}$$

$$v\varepsilon_p = \sqrt{\frac{1}{N_S}\sum_{j=1}^{N_S} v\kappa_{(p,j)}^2} \qquad \{j \in S; p \subset P\} \qquad \textbf{(13)}$$

$$v\tau_p = \sqrt{\frac{1}{n_p}\sum_{i=1}^{n_p} v\kappa_{(i,S)}^2} \qquad \{i \in p \subset P\} \qquad \textbf{(14)}$$

Unevenness and Unrepeatability Factors. Overall and regional factors are determined by dividing the square of the respective unevenness or unrepeatability value by the sum of the squares of both unevenness or unrepeatability values.

$$\mathrm{E} = \frac{v\mathrm{T}^2}{v\mathrm{E}^2 + v\mathrm{T}^2} \qquad \varepsilon_p = \frac{v\varepsilon_p^2}{v\varepsilon_p^2 + v\tau_p^2} \qquad \textbf{(15)}$$

$$\mathrm{T} = \frac{v\tau^2}{v\mathrm{E}^2 + v\mathrm{T}^2} \qquad \tau_p = \frac{v\tau^2}{v\varepsilon_p^2 + v\tau_p^2}$$

where

- $v\kappa_{(P,j)}$ imprecision value for all patches for a given sheet *j*
- $v\kappa_{(p,j)}$ imprecision value for for a subset of patches for a given sheet *j*
- $v\kappa_{(i,S)}$ imprecision value for all sheets for a given patch *i*

and

- S set of all sheets in a run
- s one sheet from the set of all sheets in a run
- P set of all patches in a sheet
- p spatial subset of patches from P
- N_P number of patches in P (entire sheet) in a sheet
- n_p number of patches in p (spatial subset) in a sheet
- N_S number of sheets in the set of all sheets S in a run

4.1.7. Inaccuracy & Imprecision Directionalities

Overall Inaccuracy Directionality. Inaccuracy directionality is determined for the circumferential or axial directions by dividing the difference between most and least accuracy band values by the difference between most and least accurate region values.

$$d\delta_b = \frac{v\delta_{b\max} - v\delta_{b\min}}{v\delta_{r\max} - v\delta_{r\min}} \qquad \begin{matrix}\{b \in p_{\{a,c\}} \subset P\} \\ \{r \in p_r \subset P\}\end{matrix} \tag{16}$$

Imprecision Directionality. Run imprecision directionality is determined for the circumferential or axial directions by dividing the square of the sum of the inaccuracy values for the bands in the respective direction by the sum of the sum of the squares of the inaccuracy values for both directions.

$$d\kappa_b = \frac{\frac{1}{n_b} \times \sum_{b=1}^{n_b} v\kappa_b^2}{\frac{1}{n_a} \times \sum_{a=1}^{n_a} v\kappa_a^2 + \frac{1}{n_c} \times \sum_{c=1}^{n_c} v\kappa_c^2} \qquad \begin{matrix} b = \{a,c\} \\ \{c \in p_c \subset P\} \\ \{a \in p_a \subset P\}\end{matrix} \tag{17}$$

where

- $v\Delta$ overall inaccuracy value
- $v\mathrm{K}$ overall imprecision value
- $v\delta_p$ regional inaccuracy value for a subset of patches p
- $v\kappa_p$ regional imprecision value for a subset of patches p

and

- p spatial subset of patches from P
- p_x subset of p in the region or band of interest
- p_r subset of p in the set of mutual regions or bands
- n_r number of partitions in the set of mutual regions
- n_b number of partitions in the set of mutual bands
- n_a number of partitions in the set of axial bands
- n_c number of partitions in the set of circumferential bands

4.2. Color Models

4.2.1. Color Measurement

CIE-Y from Spectral Curves. CIE-Y luminance calculated from spectral reflectance.

$$Y = \sum_{\lambda=360}^{780} R(\lambda) \times W_Y(\lambda) \qquad \textbf{(18)}$$

where

λ wavelength in nanometrs (nm)

$R(\lambda)$ reflectance factor at wavelength λ

$W_Y(\lambda)$ weighting factor at wavelength λ for CIE Y

CIE-L from CIE-Y*. CIE-L* lightness calculated from CIE-Y luminance.

$$L^* = 116\left[f\left(Y/Y_n\right)\right] - 16 \qquad \textbf{(19)}$$

$$f\left(Y/Y_n\right) = \begin{cases} \left(Y/Y_n\right)^{1/3} & \text{when } Y/Y_n > \left(\dfrac{6}{29}\right)^3 \\ \dfrac{841}{108}\left(Y/Y_n\right) + \dfrac{4}{29} & \text{when } Y/Y_n \leq \left(\dfrac{6}{29}\right)^3 \end{cases}$$

where

Y CIE-Y luminance of the sample

Y_n CIE-Y luminance of the illuminant (white-point)

*ISO Visual Density from CIE-L**. Visual density calculated CIE-L* lightness.

$$D_v = -\log\left[\frac{1}{116}\left(16 + L^*\right)\right]^3 \qquad \textbf{(20)}$$

CIE-L from ISO Visual Density*. CIE-L* lightness calculated from ISO Visual Density.

$$L^* = \left[116/10^{(D_v/3)}\right] - 16 \qquad \textbf{(21)}$$

where

D_v density value through the ISO Visual filter

L^* CIE-L^* under normal viewing conditions

4.2.2. Color Difference

Delta-D Density Difference. Difference between two density values D_1 and D_2.

$$\Delta D = D_2 - D_1 \tag{22}$$

Delta-L Lightness Difference*. Difference between two lightness values L^*_1 and L^*_2.

$$\Delta L^* = L^*_2 - L^*_1 \tag{23}$$

where

D_1	density value for the reference
D_2	density value for the sample
L^*_1	CIE-L* value for the reference
L^*_2	CIE-L* value for the sample

4.3. Additional Models

4.3.1. Descriptive Statistics

Arithmetic Mean. Central tendency for a sample set, including or excluding outliers.

$$\bar{x} = \frac{1}{n}\sum_{i=1}^{n} x_i \quad \textbf{(24)}$$

Sample Standard Deviation. Dispersion in a sample set, including or excluding outliers.

$$s = \sqrt{\frac{1}{n-1}\sum_{i=1}^{n}\left(x_i - \bar{x}\right)^2} \quad \textbf{(25)}$$

where

x_i value from the set of samples

n number of elements in the set of samples

4.3.2. Uniformity

Rech's Degree of Unevenness. Degree of unevenness (or Ungleichförmigkeitsgrad) based on the range between lighter and darker values relative to the mean of all samples.

$$\eta = \frac{z_{\max} - z_{\min}}{z_{avg}} \times 100\% \quad \textbf{(26)}$$

where

$z_{\max}$ density value for darkest measurement

$z_{\min}$ density value for lightest measurement

z_{avg} mean density value for all measurements

Chapter 5
Testing Method

This chapter covers the testing and analysis methodologies developed in this study for lithography and electrophotography presses with different formats and orientations.

Testing the uniformity of a printing system requires thorough sampling of the printing density for solids and halftones across the spatial and temporal domain. For this study, testing was conducted by measuring a sample of 56 impressions of a special test form adapted to the format and orientation of each press. The samples were taken from a set of 200 consecutive impressions using a mixed strategy yielding both sequential and random subsets. The special form uses a repeating checkerboard pattern including solid, quarter- and mid-tones, and, paper patches in one or more targets covering the printing plane. The targets are designed for measurement using an automated spectrophotometer.

The printing uniformity metrics, defined in *Chapter 4*, are used to analyze the data from all 56 prints for each test case. This involves converting spectral data to a measure of printing density, which may be ISO visual density (recommended) or any other optical intensity measure like CIE-L*, which is more perceptually scaled. Software was used to minimize human error and eliminate redundant data through direct instrument interface.

5.1. Test Form Design

The design of the test form is critical to the quality of the uniformity fingerprint, more so for the spatial than the temporal domain. The design must address sampling resolution, patch diversity, systematic interferences, human error, and system factors.

5.1.1. Design Procedure

Stage 1. Construction:

1. Determine sampling constraints, i.e., patch diversity and resolution.
2. Determine instrumentation constraints.
3. Design layout for the test target patches, blocks and forms.

Stage 2. Validation:

4. Test the designed target using the measurement device for conformance.

Stage 3. Adaptation:

5. Determine provisional press and testing constraints.
6. Adapt layout for the each press.

5.1.2. Sampling Constraints

The capabilities of the printing system introduce key constraints on the target design. Maximum coverage is essential to the completeness of the uniformity fingerprint. The printing area dimensions, substrate specifications, and any special length considerations (e.g. ink zones) determine target dimensions target and patch frequency. *Table 1* lists the specifications for the substrates used in this study. The design of the target must address interferences commonly encountered by the industry, i.e. related to tone reproduction, unit-to-unit printing, and, ink starvation.

Table 1. Printing area and substrate specifications for actual press tests.

Pressrun	Maximum Sheet	Maximum Image	Actual Sheet
	Offset Lithography		
L0	740 × 510 mm	740 × 487 mm	635 × 483 mm
L1, L2, L3	740 × 510 mm	740 × 487 mm	635 × 483 mm
	Electrophotography		
X1	330 × 483 mm	330 × 460 mm	483 × 318 mm
X2	330 × 483 mm	317 × 464 mm	318 × 483 mm

Halftones. Tone value increase is a key aspect in many printing processes and press designs. It is common practice to append color control strips with solid patches and tints.

In order to capture both the solid and halftone uniformity profiles and address tone-related concerns the target incorporates solid, tints and slur patches, as shown in *Figure 16*. Priority was given for the sampling of solids at double the rate of sampling for the tints, which were also sampled at double the rate of paper and slur patches.

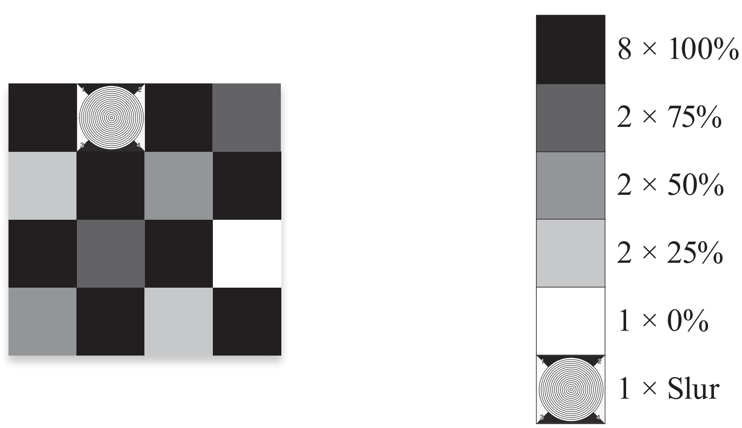

Figure 16. 16-Patch Checkerboard Test Target Repeating Block (4×4)

It is presumed that the difference in how inks and substrates interact across processes and designs may have fundamental inconsistencies between the uniformity of solids and the various tints. It is also presumed that in some cases slurring will occur which can affect tone reproduction. *Table 2* shows a tally for each test form variant.

Table 2. Test target patch count for presses L1-3 and X1-2.

Patch Type	L Count	X Count
Solid	1872	1496
Three-Quartertone	468	374
Mid-tone	468	374
Quartertone	468	374
Paper-White	234	187
Slur	234	187

Latent Image. Another common problem in some contact-printing systems is that the image content will influence the available supply of ink. If the image content is random, one may expect unpredictable non-uniformity patterns. This means that the layout of the patches may result in non-uniformity due to ink supply, which may overlap and interfere with fingerprinting the non-uniformity of the press.

To normalize the effects of ink supply and demand, it was deemed essential to layout the patches in repeating target blocks. This is not intended to eliminate latent interferences but rather synchronize them into consistent patterns. This is expected to provide a more faithful fingerprint. The consistent latent interferences may be more pronounced in some systems than others, but, this is unavoidable systematic noise.

Ink Trap. A common problem in multicolor printing in some contact-printing designs arises from the inconsistent ink transfer onto unprinted substrate versus overprinting.

To avoid such interferences, the target is design for testing printing unit individually. This is a substantial change from the multicolor test forms used in previous works (Abdel Motaal & Sikander, 2009; Breede, 2007; Sigg, 2007). The added advantage of single-unit testing is the allowance for sampling at higher resolutions.

Ink Starvation. A common problem in lithography is the inconsistent flow of ink caused by the mechanics of transporting from the fountain to the plate, which affects the uniformity of large solid areas with high ink demand. Ink starvation can be remedied by using checkerboard patches, in *Figure 17*, instead of continuous areas, to moderate demand.

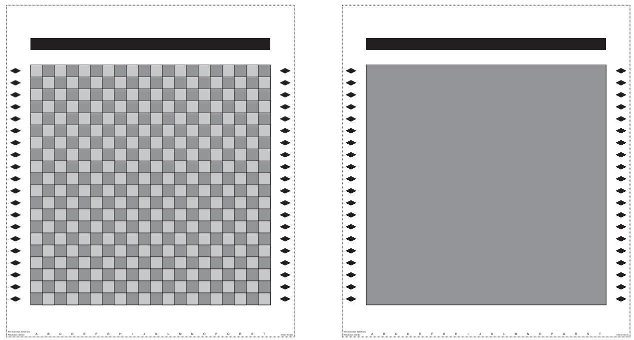

Figure 17. Checkerboard (left) versus full-coverage (right) design.

Ink Zones. The design of any printing system entails specific systematic interference patterns. For the most part, these patterns should not be treated or controlled using techniques that are not conventional to standard operating procedures. However, efforts must be made to alleviate interferences that would degrade the reliability of the fingerprint. For the lithography press, the size of the patches was optimized to synchronize with the ink zones, as shown in *Figure 18*. The target blocks and the gap between the targets were to independently reflect the profile for each ink zone.

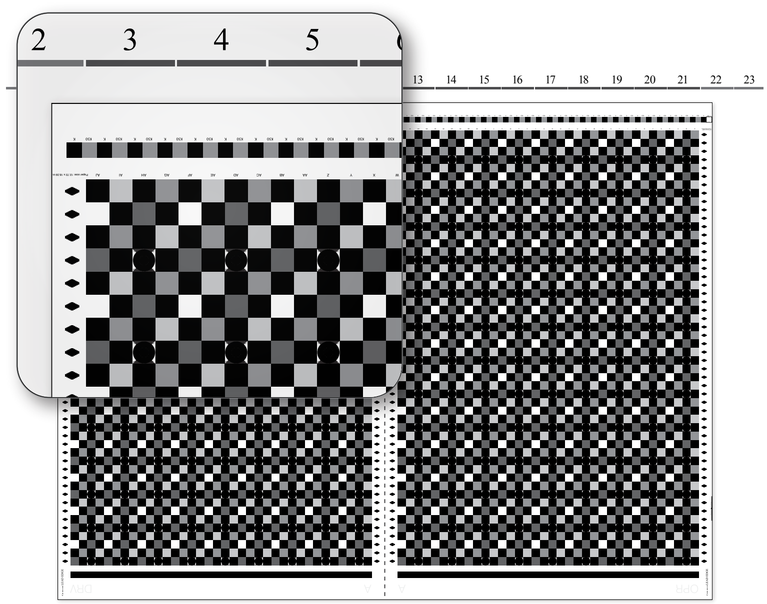

Figure 18. Alignment of patch with ink zones of the press.

5.1.3. Instrument Constraints

Measurement interference and human error are the two considerations related to instrumentation. The implications of measurement interferences are recognized however the objective of the experiment is to generate model data. This renders the measurement error factor insignificant apart from the need of using industry-grade instruments proven on the field for quality control applications.

Automated measurement is the key to limiting human error. Such automated instruments, i.e. the X-Rite Eye-One iSis XL spectrophotometer which is recommended, place certain design constraints. This in some cases requires tiling several targets on the test form to fingerprint presses with larger formats than supported by the instrument.

The target design specifications for the automated spectrophotometer require the incorporation of whitespace and special elements including track marks, illustrated in *Figure 19.* Limiting criteria are specified regarding the patch size (6-20 mm) and patch count (up to 3000 patches), and, target dimensions (maximum 66 cm × 33 cm). This includes a feeding lead-edge margin (minimum 331 mm), side margins for the track marks (minimum 11 mm), and, a trail-edge margin (minimum 250 mm) (X-Rite, 2007).

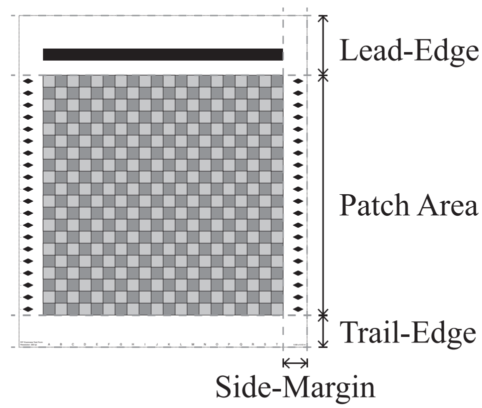

Figure 19. Eye-One iSis target design features (adapted form X-Rite, 2007).

5.2. Sample Production & Measurement

Printing Procedures. Separate workflows are used for each printing process as follows.

Lithography Printing Workflow:

1. Design and customized test form layout and ensuring conformance.
2. Generate identical printing plates for the three runs.
3. Clean up the press and prepare the ink and load the substrate.
4. Replenish the ink fountain and load the printing plate.
5. Make-ready the press to a stable condition following standard procedures.
6. Run a minimum buffer of 200 sheets after the OK print before collecting samples.
7. Run 300 additional prints after the buffer for sampling according to *5.2.1.*

Electrophotography Printing Workflow:

1. Design and customized test form layout and ensuring conformance.
2. Clean up the press and load the ink and substrate.
3. Make-ready the press to a stable condition following standard procedures.
4. Run a minimum buffer of 200 sheets after the OK print before collecting samples.
5. Run 300 additional prints after the buffer for sampling according to *5.2.1.*

5.2.1. Sheet Selection

Sampling Procedures. The procedure includes two strategies from a 200-sheet sample. The procedure is repeated for every pressrun and the sequence of the sheets must be marked on sheet for 200-sheet set.

First Sequential Sample:

1. Select and label the first 10 consecutive prints from the 200 good prints.

Quasi-Random Sample:

2. Select and label a random sheet for every 5 sheets for a total of 36 sheets between sheets 11 and 190 from the 200 good prints preserving the sequence of the sheets.

Second Sequential Sample:

3. Select and label the last 10 consecutive prints from the 200 good prints.

5.2.2. Measurement

The sample prints were measured using the automated spectrophotometer to derive the commonly used densitometric and colorimetric values.

Instrumentation. The measurement method was designed to limit both human and instrument error for the very large number of readings, which included hundreds of prints and close to a million individual patches. This was achieved through the use of an industry-grade automated sheet-fed spectrophotometer.

Workflow. The exceptionally large scale of measurements required developing special MatLab software to interfaces directly with the spectrophotometer. This software ensures efficient well-structured data collection through a semi-automated systematic process.

Data. A MatLab-based software was used to measure and separately store spectral reflectance data for all the patches across all sheets for each test case. Additional processing was done to convert the spectral measurements to ISO Visual Density data ready for on demand conversion to CIE-L*, using *Equation 21*, and, real-time plotting.

Metadata. It was essential to capture and encode additional metadata together with the raw data for each test run. This included information regarding target specifications, prepress workflows, consumables, printing, sample selection, and measurement.

5.3. Data Analysis

The section explains the process of applying certain Printing Uniformity Evaluation metrics in order to generate the results needed to test the hypothesis outlined in the descriptive portion. The reader is referred to *Chapter 3* and *Chapter 4* for the full set of metrics and underlying concepts.

5.3.1. Data Processing

To apply the mathematical formulae for the various metrics it is essential to first process the raw data generated in the measurement process in section *5.2.2*, which includes two main stages. First, processing of the metadata is conducted to determine the layout of the patches and generate regional masks for the different groups, including regions, bands, and ink zones where applicable. Second, the data is filtered using the masks then used to compute the final results, including all run and regional metrics.

Chapter 6
Results and Findings

This chapter presents the results and findings for five test runs executed in this research to develop, refine and exemplify the framework, models and method proposed.

6.1. Pressruns

Five pressruns were conducted for this study focusing on of lithography and electrophotography presses. Two electrophotography presses were each tested using a single run, totaling two runs, referred to as X1 and X2. Two lithography units from the same press were tested and the first of those units was retested, totaling three runs, referred to as L1, L2, and L3, respectively. All runs used the same substrate but the inks were of course specific to each system.

6.1.1. Printing Overview

Electrophotography Pressruns. X1 and X2 were conducted using the black printers of two 12 × 18 inch portrait presses. X1 was conducted on a model newer than X2. Both presses share the same manufacturer, brand, format, process and fundamental press design aspects. The substrate was run grain short to wrap tightly around the impression cylinder in portrait orientation, which eliminates the potential for grain to induce variability along the circumferential direction.

Lithography Pressruns. L1, L2 and L3 were conducted using single units of the same 25 × 19 inch landscape press. L1 and L3 were printed on the same printing unit of the same press using separate plates and independent make-ready after proper cleanup. The substrate was run grain long to wrap tightly around the cylinder in landscape orientation for the same considerations as for X1 and X2 above.

6.1.2. Spatial Regions

Regional metrics apply to subsets of data dividing the spatial domain into regions and bands. *Table 3* shows the various dimensional aspects for the presses used.

Table 3. Printing area and substrate specifications for actual press tests.

Pressrun	Actual Sheet	Sample Area	Bands	Region Size
L1, L2, L3	635 × 483 mm	635 × 483 mm	5 × 3	127 × 96.9 mm
X1	318 × 483 mm	318 × 483 mm	3 × 5	106 × 96.9 mm
X2	318 × 483 mm	318 × 483 mm	3 × 5	106 × 96.9 mm

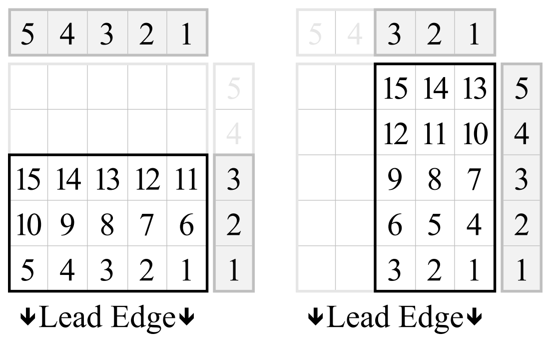

Figure 20. Regions and bands maps for runs L1-3 (left) and X1-2 (right).

Regions refer to equally sized areas dividing the printing plane into a grid of rows and columns with an almost square ratio between the vertical and horizontal dimensions, respectively. Regions are labeled using the prefix R, as shown in *Figure 20.*

Bands refer to equally sized areas dividing the printing plane into either rows or columns with the same respective vertical and horizontal dimension of the regions grid, respectively, for the circumferential and axial directions. Bands are labeled using the prefix A for axial and C for circumferential, as shown in *Figure 20.*

The layout in *Figure 20* is used throughout this chapter to present metrics for regions and bands in the respective cells and the run metrics in the top right corner.

6.2. Printing Uniformity Metrics

Printing uniformity metrics relate to the indicators addressing the overall and regional constructs for both the printing accuracy and printing precision dimensions.

6.2.1. Printing Accuracy Metrics

Printing accuracy is quantified using overall and regional scores, proportions and directionalities, as shown in *Figure 21*. Inaccuracy values represent central tendency error of for the entire run or within regions and bands excluding outliers, relative to a reference aim point for the entire run and to the mean of the run for regions and bands.

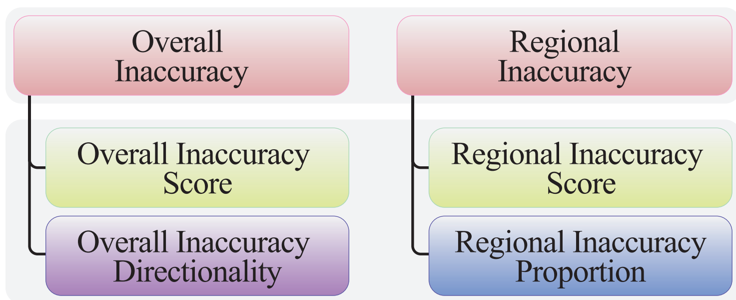

Figure 21. Printing accuracy constructs and indicators.

Inaccuracy scores are derived from inaccuracy values relative to predefined tolerance. These scores represent the inaccuracy normalized to the defined tolerance using percent notation starting at 0% and may reach and pass the −100% mark relative to the tolerance. An inaccuracy score of zero means no deviation, a score of 100% or above means that the deviation is equal or greater than the tolerance.

Inaccuracy proportions are derived from the inaccuracy values of region or bands. These proportions represent the extent by which bands or regions contribute to the total inaccuracy, which may reveal bias patterns. Proportioning is exclusive to each regional subset or grouping where the proportions for all the regions, all axial bands, or, all the circumferential bands will total 100% separate from other regional subsets.

Inaccuracy directionalities are based on the range of inaccuracy values between the best and worst axial or circumferential bands against the range for regions by adapting Rech's formula (*Equation 26*). Directionality pairs represent the tendency to which inaccuracy aligns with the circumferential or axial direction, irrespective of the extent of bias. Difference in directionalities suggests alignment to the higher value, while close values suggest no tendency for alignment.

6.2.2. Printing Precision Metrics

Printing precision is quantified using scores, proportions, and directionalities, as well as unevenness and unrepeatability factors, in *Figure 22*. Imprecision values represent the six-sigma overall, in regions and bands as with inaccuracy.

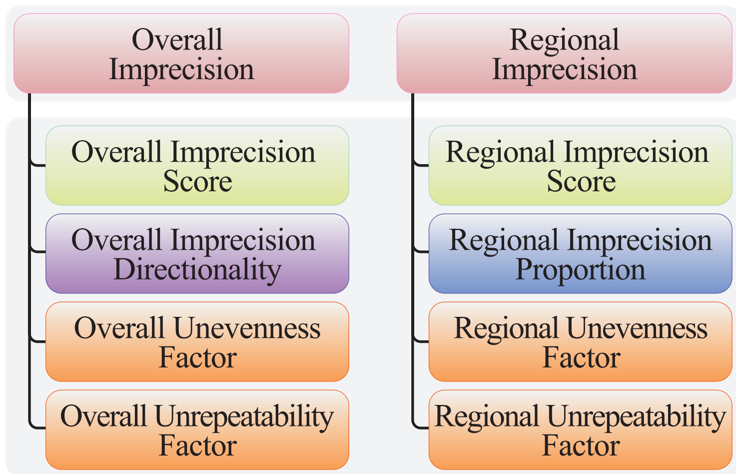

Figure 22. Printing imprecision constructs and indicators.

Imprecision scores are derived fromw imprecision values relative to predefined tolerance. These scores represent the imprecision normalized to the defined tolerance using percent notation starting at 0% and may reach and pass the −100% mark relative to the tolerance. An imprecision score of zero means no variation, a score of 100% or above means that the variation is equal or greater than to the tolerance.

Imprecision proportions are derived from imprecision values of region or bands. These proportions represent the extent by which regions and bands contribute to the total imprecision, which may reveal non-uniformity hotspots. Proportioning is exclusive to each regional subset or grouping where the proportions for all the regions, all axial bands, or, all the circumferential bands will total 100% separate from other regional subsets.

Imprecision directionalities are derived from weighted ratios for the sum of the squares for axial or circumferential bands. These directionality pairs represent the extent to which variability is aligned with the circumferential or axial direction, irrespective of the extent of variability. They only signify the tendency for any potential variability to be directionally aligned. Equal directionalities suggest no tendency for alignment. A higher directionality suggests some tendency for alignment in the respective direction.

Unevenness and unrepeatability factors are derived from imprecision values along the respective domains also using the weighted ratios for the sum of squares for patches and sheets. These factors represent the tendency for spatial unevenness in the sheets or the temporal unrepeatability patches. These factors apply exclusively to imprecision.

6.3. Analysis of Overall Uniformity

In order to better understand the metrics presented, it is important to go back to basics and look at statistical distributions. To help bridge concepts, statistics for solid-ink density are presented prior to the various metrics covering solids, quartertones and paper. Complete tables and figures covering the entire set of metrics for all the pressruns and all the tone levels are provided in the appendix**.**

6.3.1. Overall Inaccuracy

Figure 23 shows the distribution of the absolute density for all the solid patches with vertical lines indicating the mean densities. It can be observed that the means vary widely, far from the aim point, and that they do not align with the peaks.

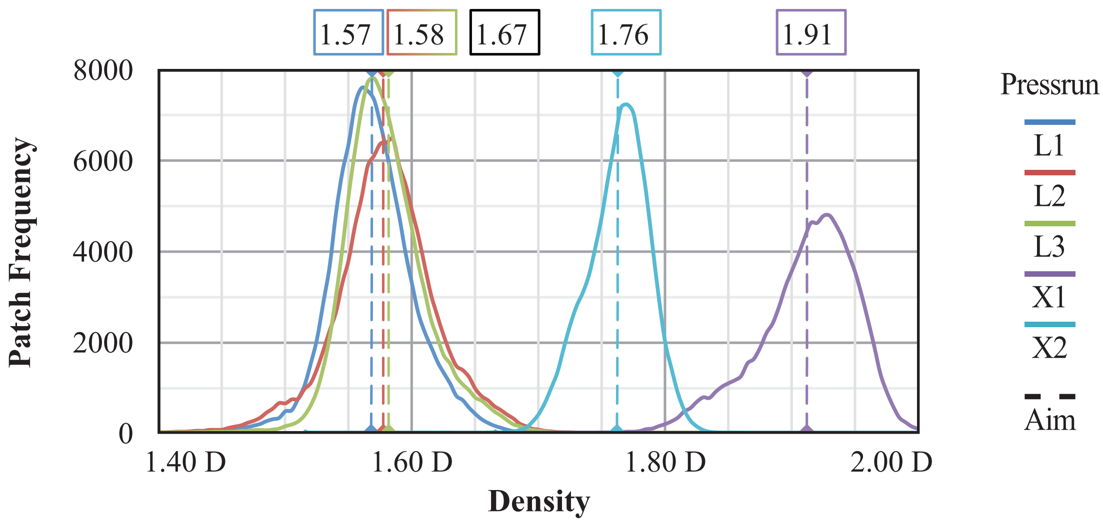

Figure 23. Solid-ink density distributions for all runs versus aim point.

Solid-ink distributions show only a part of the picture. There is no indication or guarantee that the inaccuracy trends for solids will predict the accuracy of halftones.

Many processes use semi-opaque or translucent inks. As such, observations regarding printing accuracy for solids and halftones become less appropriate without knowing how the paper is skewing the results. Moreover, halftones are subject to tone value increase; where ink-and-paper interactions will yield darker tones on paper than intended. This may present differently on different presses. Hence, paper and halftones must be taken into consideration.

6.3.2. Run Inaccuracy Score

Run inaccuracy values in *Table 4* compare the mean for solids, halftones and paper for the entire run, i.e. includes every patch on every sheet, relative to the aim point.

Table 4. Run inaccuracy values for all five pressruns across tone values.

Pressrun	TV100	TV75	TV50	TV25	Paper	
L1	-0.107	-0.043	+0.018	+0.029	+0.019	D
L2	-0.096	-0.022	+0.027	+0.030	+0.019	D
L3	-0.096	-0.038	+0.019	+0.028	+0.016	D
X1	+0.237	+0.015	+0.035	+0.029	+0.018	D
X2	+0.087	+0.026	+0.036	+0.029	+0.014	D

Run inaccuracy scores in *Table 5* are derived from inaccuracy values to indicate the ratio of inaccuracy weighted against ±0.05 D tolerance for all tones and ±0.025 D for paper. Inaccuracy scores reflect degraded accuracy irrespective of direction.

Table 5. Run inaccuracy scores for all pressruns across tone values.

Pressrun	TV100	TV75	TV50	TV25	Paper	
L1	-215	-86	+37	+59	+76	%
L2	-192	-43	+54	+61	+75	%
L3	-192	-75	+38	+56	+65	%
X1	+473	+30	+71	+57	+72	%
X2	+174	+52	+71	+58	+58	%

Since inaccuracy score are relative to allowed tolerance, any score beyond the ±100% mark reflects inaccurate by more than one-times the tolerance. Moreover, these scores are comprehensive enough for reliable comparisons, as shown in *Figure 24*.

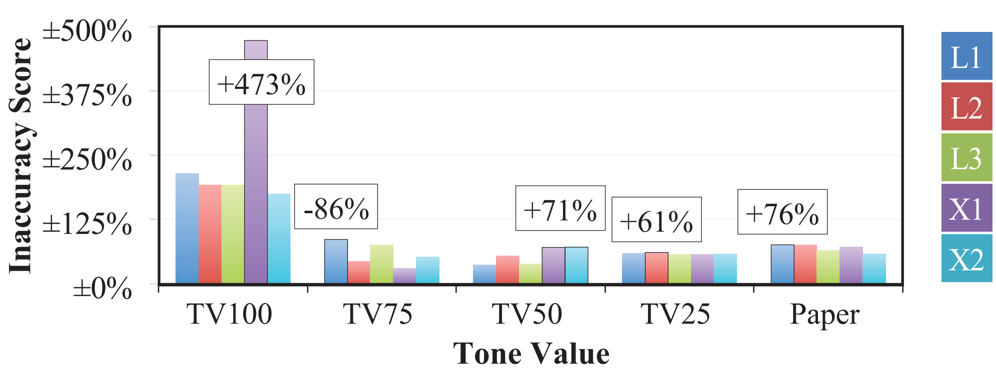

Figure 24. Overall inaccuracy scores across all tone values for all presses.

6.3.3. Overall Imprecision

Figure 25 shows the distribution of density for all solid patches relative to the mean densities of each run with vertical lines indicating the allowed tolerance. It can be observed that the distributions distinctively vary between presses and between units.

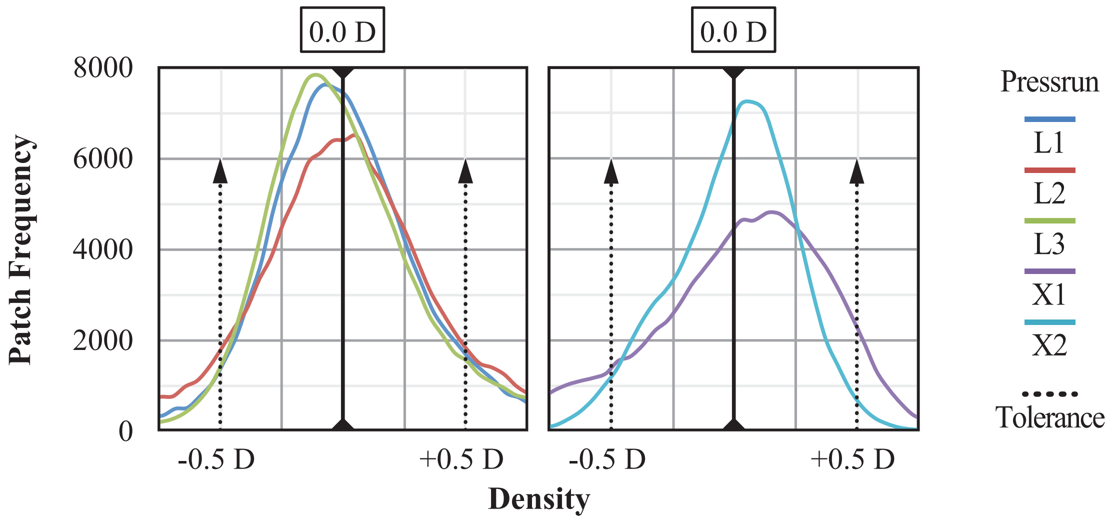

Figure 25. Relative solid-ink density for L1-3 (left), and, for X1-2 (right) and tolerance.

Similarities and differences between the lithography runs, L1, L2 and L3, versus the electrophotography X1 and X2 can be seen clearly in the shape of the curves around the means. Greater differences can be observed between the electrophotography runs than with the lithography runs. It is also observed that L2, from press 1 unit B, has a distinct shape from L1 and L3, both from press 1 unit A, which are very similar.

Essentially, we can expect tall and narrow distributions with well-centered peaks to be more precise than wider distributions or ones that are less normally distributed. Statisticians rely on other descriptive measures to describe the shape of the distribution, e.g. skewness, which describes the slant of the peak relative to the base, and kurtosis, which describes the relative proportions of the peak, shoulder and tail. Generic statistical measures may provide objective comparable data regarding the shape of the curve. However, the shape of the curve is not the problem but rather one possible solution.

The problem at hand is to provide a measure of the printing precision. This may be solved through scores that would describe the extent for imprecision, in the following section, which would also be tied to other metrics that provide objective and comparable measures regarding the contributory significance of critical subsets. The latter is covered in sections *6.4.8* and *6.4.4* addressing spatial-temporal and regional subsets.

6.3.4. Run Imprecision Score

Run imprecision values in *Table 6* reflect the dispersion for the entire run which are fundamentally six-sigma, i.e. six-times the standard deviation.

Table 6. Run imprecision values for all five pressruns across tone values.

Pressrun	TV100	TV75	TV50	TV25	Paper	
L1	0.200	0.084	0.052	0.030	0.020	D
L2	0.236	0.129	0.052	0.026	0.018	D
L3	0.192	0.086	0.049	0.027	0.018	D
X1	0.233	0.147	0.082	0.049	0.011	D
X2	0.148	0.089	0.063	0.036	0.011	D

Run imprecision scores, in *Table 7*, are derived from imprecision values to indicate the ratio of the imprecision weighted against ±0.05 D tolerance for all tones and ±0.025 D for paper. Both imprecision values and scores have no direction.

Table 7. Run imprecision scores for all pressruns across tone values.

Pressrun	TV100	TV75	TV50	TV25	Paper	
L1	200	84	52	30	40	%
L2	236	129	52	26	36	%
L3	192	86	49	27	37	%
X1	233	147	82	49	22	%
X2	148	89	63	36	22	%

Since imprecision score much like inaccuracy scores are relative to allowed tolerance, scores beyond ±100% reflect imprecision by greater than the tolerance. These scores also are comprehensive enough for reliable comparisons, as shown in *Figure 26*. When imprecision and inaccuracy scores are combined they can reflect the extent of variability for printing systems in relative terms, making it easier to compare systems.

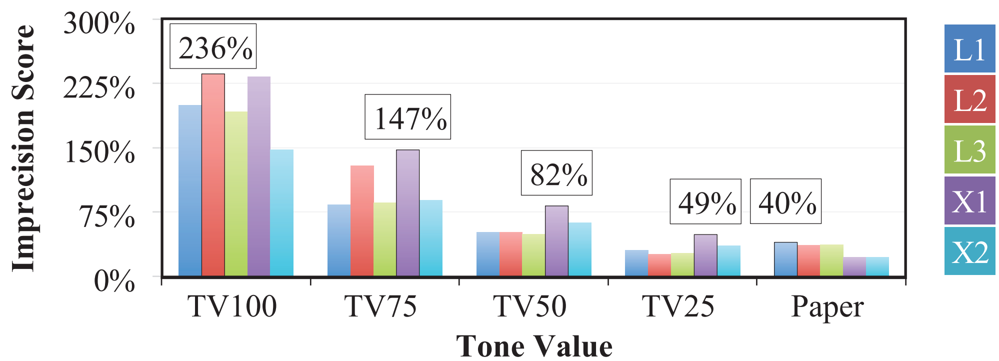

Figure 26. Run imprecision scores across all tone values for all presses.

6.3.5. Unevenness and Unrepeatability Factors

Figure 27 compares the significance the orthogonal spatial-temporal dimensions on observed imprecision, reflecting unevenness versus unrepeatability. Factors are expressed as the ratio of temporal and spatial factors, as shown in *Table 8*. The two ratios represent 100% of the imprecision indicated by the imprecision score.

Table 8. Run unevenness and unrepeatability factors for all tone values.

Pressrun	TV100	TV75	TV50	TV25	Paper	
L1	24:76	38:62	45:55	49:51	44:56	%
L2	15:85	14:86	28:72	35:65	39:61	%
L3	16:84	25:75	31:69	27:73	33:67	%
X1	19:81	14:86	17:83	20:80	48:52	%
X2	55:45	25:75	20:80	23:77	47:53	%

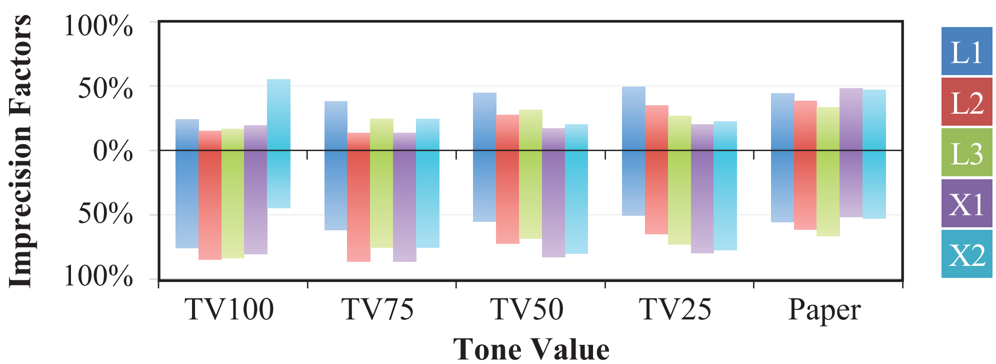

Figure 27. Unevenness versus unrepeatability factors for all runs.

A lot more observations can be made by looking at *Figure 27*, which could not be illustrated in the distribution histograms in *Figure 25*. It can be observed that regardless of the biases for all pressruns at TV100% all runs seem to somewhat level out for the paper. Another aspect is that this trend seems to be gradual from the solids through to the paper for L1, L2 and L3 but hold steady and trasnition abruptly between TV25% and for X1 and X2. A possible explaination can be in the fact the X1 and X2 use liquid toner which tends to be more opaque then conventional offset inks.

X2 has an anlomoly where it abruptly transition from balanced ratios at TV100% to strong spatial bias for all halftones. This is not seen in X1 or any other runs for that matter. This may suggest that the quality of the halftone dots for X2 is not consistent along the spatial domain, but that this variability is consistent between impressions. However, regional factors must be analyzed in order to make decisive observations and not merely conjecture. This is covered in section *6.5.2*.

6.4. Analysis of Regional Uniformity

6.4.1. Regional Inaccuracy

The underlying idea behind overall inaccuracy can be extended to regions and bands. However, regional inaccuracy scores indicate inaccuracy relative to the mean for each run rather than to the aim point. *Figure 28* shows density distribution for entire runs versus subsets for three evenly spaced bands dividing the short dimension, which is circumferential for landscape presses L1, L2 and L3, and, axial for portrait X1 and X2.

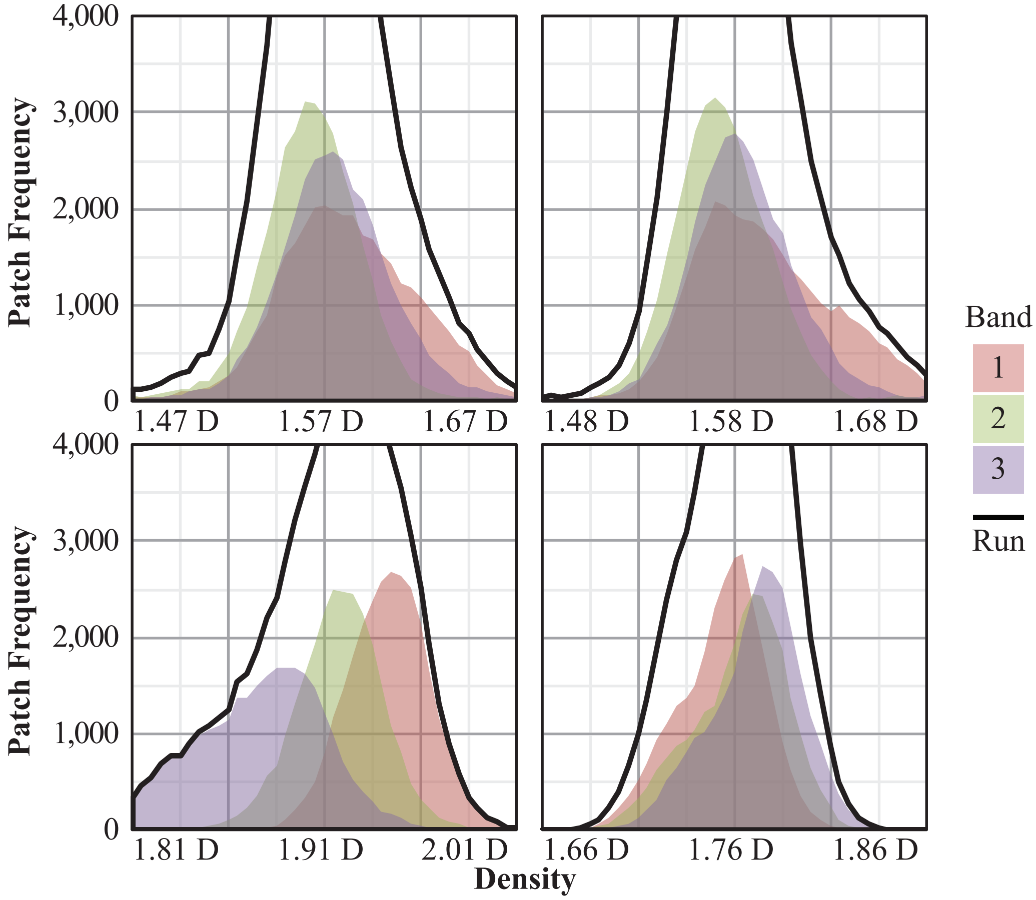

Figure 28. Density for L1 & 3 (top) circumferential and X1 & 2 (bottom) axial bands.

Regional inaccuracy influences both the overall inaccuracy and overall imprecision, as shown in *Figure 28* above. Contrasting the similarities and differences of the overall shapes relative to the clusters of the subsets can further elaborate this relationship. It is clear that the shapes of the overall curves (black lines) for L1 and L3 are very similar to one-another whereas the shapes for X1 and X2 are different. Inherently, clusters with closer central tendencies result in narrower the overall curves.

Although it was practical to look at the distributions when showing only three subset clusters for each printer, it becomes a lot more difficult with a larger number of clusters. *Figure 29* shows subsets for X1 and X2 as in *Figure 28*, but this time dividing bands around the cylinder.

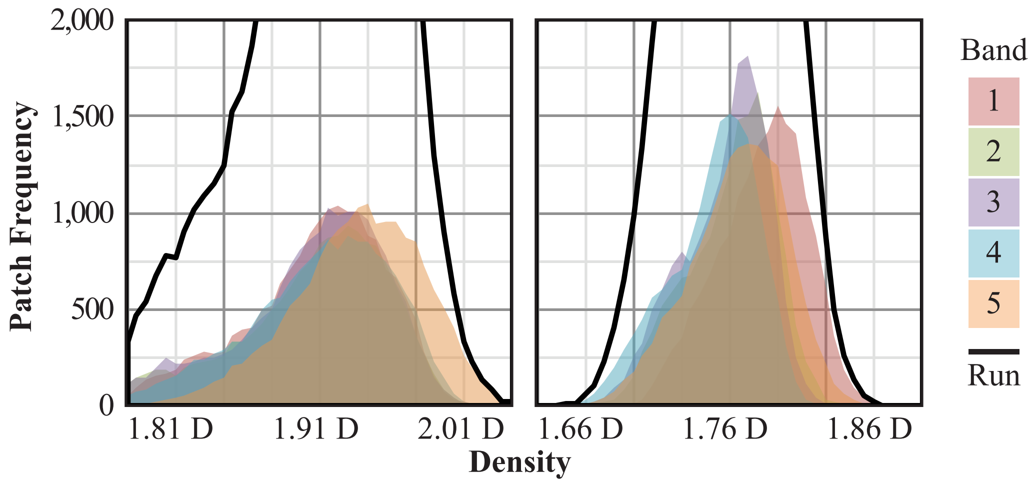

Figure 29. Density for circumferential bands for X1 & X2 using filled curves.

Figure 30 shows the same curves for X1 and X2 in *Figure 29*, but these curves are plotted as outlines instead of filled areas.

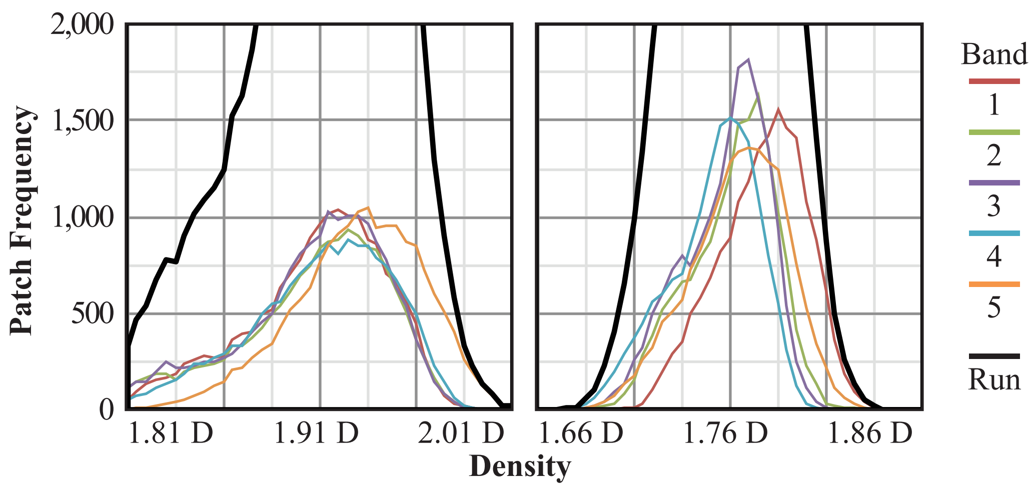

Figure 30. Density for circumferential bands for X1 & X2 using outlined curves.

Given the overload of features, can we draw any practical conclusions from distribution plots if we increased the number of subsets from three to five? With large numbers of subsets there is way too much detail, which makes it very appealing to make assumptions and a lot harder to look objectively for trends in the data.

Although there is something to be said about the influence of the visual style attributes of the plots, the bottom-line is cluttered histograms enable the reader to notice features that are more perceptible to them based on biases from their experience. Essentially, this only gets grimmer when trying to conceive look at even larger subsets, like regions. Since regions are the intersecting subdivisions of axial and circumferential bands, they would end up generating fifteen region clusters and fifteen curves to look at.

From this, it can be safely assumed that distribution plots are not suitable to for making complete and reliable observations regarding printing uniformity. Distribution plots may be well suited and popular for other applications.

To overcome the challenges regarding printing uniformity we can consider using metrics for capturing the key features for each subset in a more practical and objective manner. Such metrics are an essential first step in order to help describe and visualize this very specific phenomenon. In the case of regional inaccuracy, scores that compare the inaccuracy of the means of each subset relative to the tolerance may provide the necessary solution to the problem.

6.4.2. Region Inaccuracy Score

Region inaccuracy scores are derived from inaccuracy values to indicate the ratio of inaccuracy against ±0.05 D tolerance for all tones and ±0.025 D for paper, providing more intuitive representation. Region inaccuracy values compare mean of the subset within the region against the mean of the entire run.

Inaccuracy values for most and least accurate regions are in *Table 9 and Table 10.* Inaccuracy scores for the same regions are in *Table 11 (pp. 65)* and *Figure 31.*

Table 9. Most accurate region inaccuracy values for all runs.

Pressrun	TV100	TV75	TV50	TV25	Paper	
L1 [R13]	-0.0016	+0.0019	+0.0045	+0.0007	-0.0002	D
L2 [R13]	-0.0005	+0.0007	+0.0005	-0.0006	-0.0004	D
L3 [R1]	-0.0003	-0.0034	-0.0017	-0.0011	-0.0010	D
X1 [R8]	+0.0017	+0.0080	+0.0047	+0.0034	-0.0010	D
X2 [R5]	-0.0011	-0.0058	-0.0002	+0.0010	-0.0007	D

Table 10. Least accurate region inaccuracy values for all runs.

Pressrun	TV100	TV75	TV50	TV25	Paper	
L1 [R4]	+0.0248	+0.0137	+0.0093	+0.0049	+0.0028	D
L2 [R6]	-0.0477	+0.0195	+0.0088	+0.0043	+0.0031	D
L3 [R8]	-0.0287	+0.0144	+0.0097	+0.0047	+0.0034	D
X1 [R6]	-0.0480	+0.0214	+0.0115	+0.0067	+0.0019	D
X2 [R3]	+0.0264	+0.0154	+0.0091	+0.0052	+0.0019	D

Numbering of the bands and regions in the tables above and in following tables all refer to the layout presented in *Figure 20 (pp. 53)*, which is presented again below.

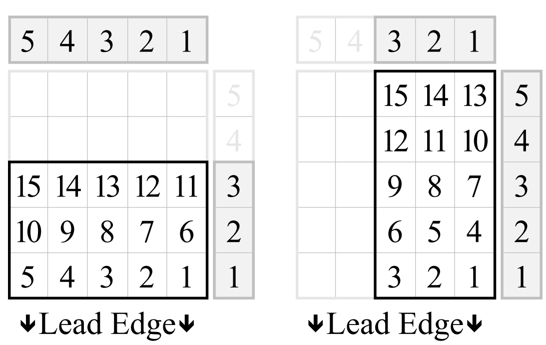

Figure 20 (repeated). Regions and bands maps for runs L1-3 (left) and X1-2 (right).

Region inaccuracy scores for most accurate regions provide the extent of accuracy whereas least accurate regions signify the extent of inaccurate. There is practical value in knowing the upper and lower limits especially when color is critical.

Table 11. Most versus least accurate region inaccuracy scores.

Pressrun	TV100		TV75		TV50		TV25		Paper		
L1 [R13 - R4]	-3	+50	+4	+27	+9	+19	+1	+10	-1	+11	%
L2 [R13 - R6]	-1	-95	+1	+39	+1	+18	-1	+9	-2	+12	%
L3 [R1 - R8]	-1	-57	-7	+29	-3	+19	-2	+9	-4	+14	%
X1 [R8 - R6]	+3	-96	+16	+43	+9	+23	+7	+13	-4	+8	%
X2 [R5 - R3]	-2	+53	-12	+31	0	+18	+2	+10	-3	+8	%

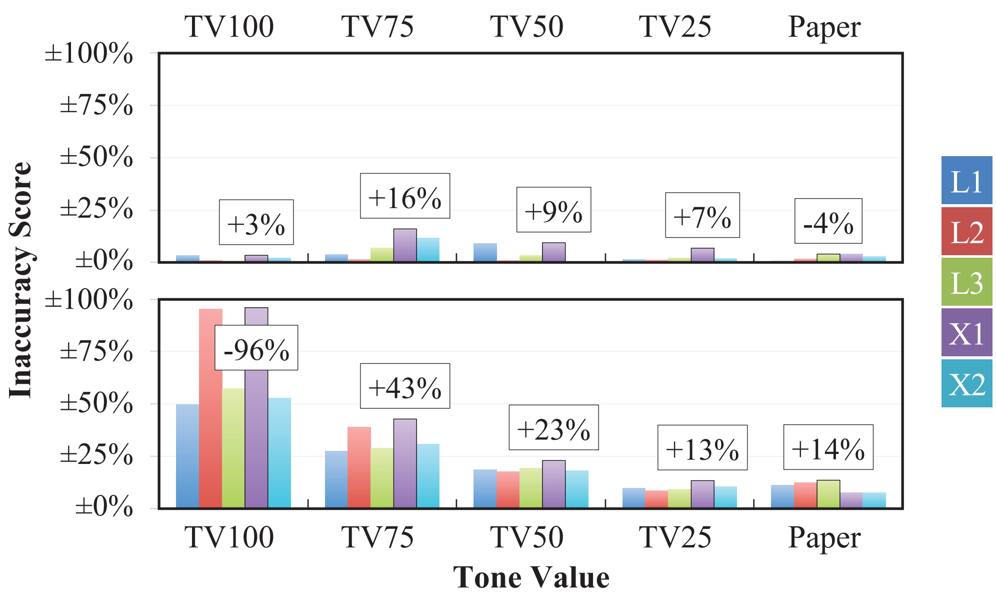

Figure 31. Region inaccuracy scores for most (top) and least (bottom) accurate regions.

It is clear in *Figure 31* that the region accuracy limits differ largely between presses, processes and even between press units. From *Table 11*, X1 ranks as the worst press based on the range in inaccuracy scores in the most and least accurate regions, scoring between 3% and 96% irrespective of direction for solid patches. X2 is much more accurate across the regions, between 2% and 53%. This is comparable to L1 and L3, which were printed on the same printing unit, between 3% and 50% for L1 and 1% to 57% for L3. L2 falls second worst, between 1% and 95%, which compares with X1. One final point to note is that the most and least accurate regions for solid patches are not necessarily the same for the quartertones and paper. Solids provide the strongest representation for the printing accuracy since it holds the highest ink coverage.

6.4.3. Circumferential and Axial Band Inaccuracy Score

Band inaccuracy values and scores are similar to regions, however the subset includes patches along either rows or columns, respectively, for each direction. *Table 12* shows scores for the least accurate circumferential and axial bands.

Table 12. Least accurate circumferential and axial band inaccuracy scores.

Pressrun	TV100		TV75		TV50		TV25		Paper		
L1 [C2 - A1]	-20	-28	+167	+169	+103	+113	+61	+64	+79	+85	%
L2 [C1 - A1]	+26	-74	+258	+194	+103	+94	+52	+47	+72	+74	%
L3 [C1 - A5]	+22	+35	+172	+181	+98	+109	+53	+58	+74	+75	%
X1 [C5 - A3]	+35	-74	+295	+272	+164	+164	+98	+96	+44	+45	%
X2 [C1 - A1]	+29	-18	+177	+185	+125	+128	+72	+75	+44	+46	%

Insights. Just like statistical plots, there is only so much information that can be represented using this tabular format. Even the bar plots are limited in the amount of detail as well as practical use. There is a need for a representation that can provide comprehensive details in a single snapshot. This is demonstrated in sections 6.5.1 and 6.5.2 below. Complete tables and figures covering the entire set of metrics for all the pressruns and all the tone levels are provided in the appendix.

6.4.4. Regional Imprecision

The underlying idea behind overall imprecision can be extended to regions and bands. *Figure 32* shows the stacked distributions for all fifteen regions.

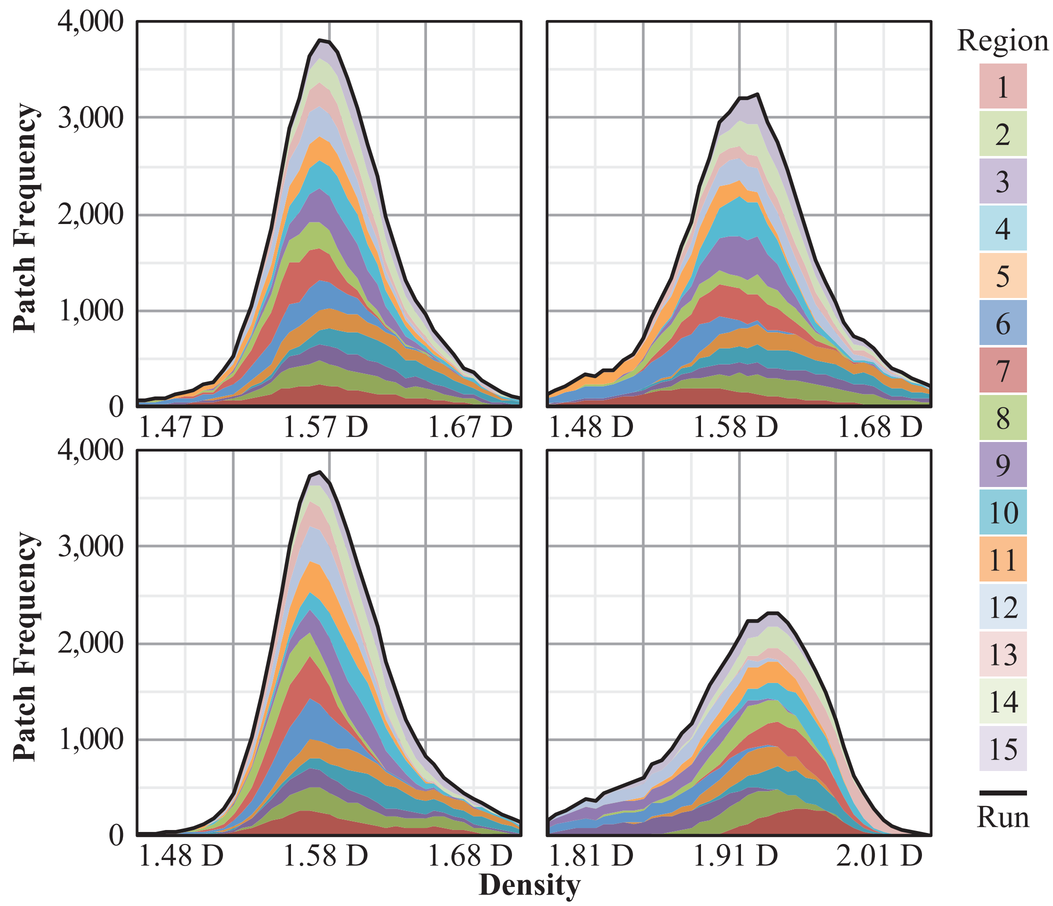

Figure 32. Stacked distributions for L1 (top-left) and L2 (top-right), L3 (bottom-left) and X1 (bottom-right).

Regional imprecision influences overall imprecision. Wider more dispersed region distributions will present a wider overall distribution. Higher region peaks signify higher precision, which will improve overall precision when the peaks are closely centered. This is shown in *Figure 32* when comparing regions and the overall curves for L2 against both L1 and L3. The regions for L2 are more dispersed than L1 and L3, which is evident in the shorter heights for the regions at their peaks. For X1, the dispersion of the regions seems to alternate from extremely wide and short to somewhat narrower tall distributions.

6.4.5. Region Imprecision Score

Region imprecision values reflect the dispersion of the subset for each region. Region imprecision scores are derived from region imprecision values to indicate the ratio of the imprecision weighted against ±0.05 D tolerance for all tones and ±0.025 D for paper. Region imprecision values for the most and least precise regions are shown in *Table 13 and Table 14*. Region imprecision scores for same regions are in *Table 15 (pp. 69)*.

Table 13. Most precise region imprecision values for all runs (Density).

Pressrun	TV100	TV75	TV50	TV25	Paper	
L1 [R7]	0.110	0.062	0.041	0.027	0.020	D
L2 [R9]	0.108	0.080	0.037	0.023	0.020	D
L3 [R7]	0.100	0.054	0.031	0.016	0.014	D
X1 [R7]	0.110	0.065	0.044	0.033	0.009	D
X2 [R3]	0.119	0.086	0.053	0.032	0.011	D

Table 14. Least precise region imprecision values for all runs (Density).

Pressrun	TV100	TV75	TV50	TV25	Paper	
L1 [R11]	0.270	0.086	0.049	0.030	0.022	D
L2 [R3]	0.293	0.128	0.042	0.022	0.012	D
L3 [R3]	0.231	0.076	0.039	0.022	0.013	D
X1 [R6]	0.202	0.127	0.067	0.041	0.011	D
X2 [R16]	0.154	0.072	0.047	0.028	0.010	D

Once again, the numbering of the bands and regions refer to the layout presented in *Figure 20 (pp. 53)*, which is presented again below.

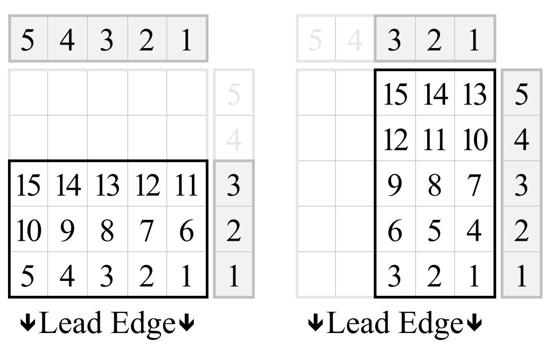

Figure 20 (repeated). Regions and bands maps for runs L1-3 (left) and X1-2 (right).

Region imprecision scores for the most precise region reflect the extent of precision, while the least precise reflect the extent of imprecision. There is practical value in knowing the upper and lower limits when accurate color is of high importance.

Table 15. Most versus least precise region imprecision scores (Percentage).

Pressrun	TV100		TV75		TV50		TV25		Paper		
L1 [R7 -R11]	110	270	62	86	41	49	27	30	40	44	%
L2 [R9 - R3]	108	293	80	128	37	42	23	22	40	24	%
L3 [R7 - R3]	100	231	54	76	31	39	16	22	27	27	%
X1 [R7 - R6]	110	202	65	127	44	67	33	41	18	22	%
X2 [R3 -R14]	119	154	86	72	53	47	32	28	22	20	%

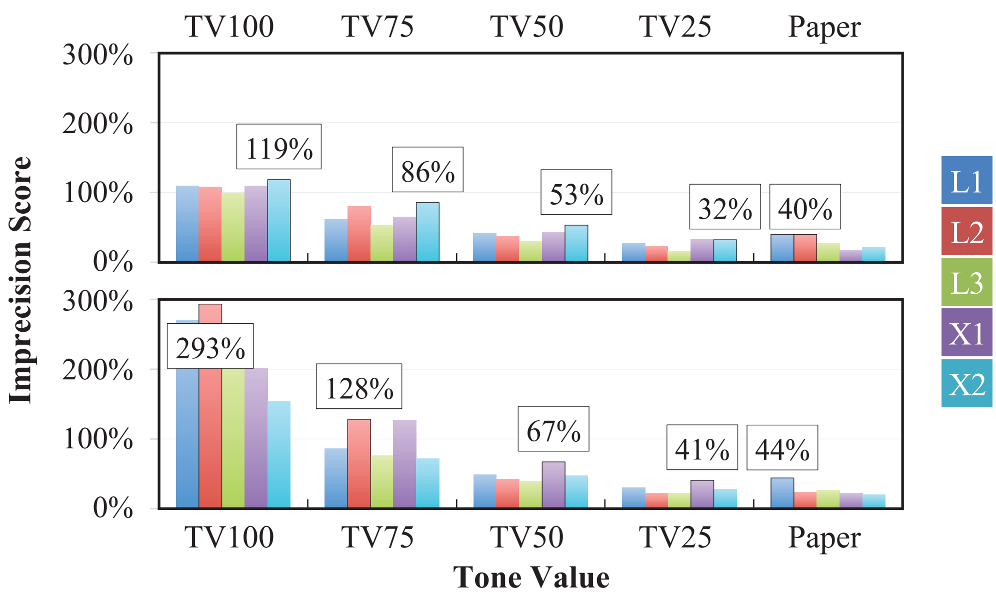

Figure 33. Region imprecision scores for most (top) and least (bottom) precise regions.

Just like region inaccuracy, region imprecision limits differ between presses, processes and units. From *Table 15*, L2 ranks the worst press based on imprecision score range, scoring between 108% and 293%. L1 and L3 follow closely with scores between 110% and 270% for L1 and 100% and 231% for L3, as shown in *Figure 33*. X1 is second best in terms of precision, between 110% and 202%. And most precise of all is X2, between 119% and 154%. Again, the locations of the most and least precise regions vary for solids, tones and paper. However, solids provide the strongest representation for the printing precision as it is holds the highest ink coverage.

6.4.6. Circumferential and Axial Band Imprecision Score

Band imprecision values and scores are similar to regions, however the subset includes patches along either rows or columns, respectively, for each direction. *Table 16* shows scores for the least precise circumferential and axial bands.

Table 16. Least precise circumferential and axial band imprecision scores (Percentage).

Pressrun	TV100		TV75		TV50		TV25		Paper		
L1 [C1 - A1]	-215	-237	-86	-85	-47	-46	-28	-28	-19	-21	%
L2 [C1 - A3]	-265	-251	-152	-117	-56	-50	-27	-24	-18	-14	%
L3 [C1 - A3]	-218	-193	-88	-64	-45	-46	-24	-22	-18	-19	%
X1 [C2 - A3]	-242	-205	-154	-128	-82	-69	-49	-40	-11	-11	%
X2 [C5 - A2]	-150	-147	-93	-67	-64	-46	-37	-27	-11	-9	%

Insights. The following sections provide a more comprehensive snapshot with a lot more details than can be represented using statistical plots, tables and bar charts. Imprecision is covered in section *6.5.2* preceded by inaccuracy in section *6.5.1.* Complete tables and figures covering the entire set of metrics for all the pressruns and all the tone levels are provided in the appendix.

6.4.7. Regional Proportions and Ranks

Ranking is achieved by sorting the region and bands based on their proportions, which were previously presented in tables for most and least precise or accuracy regions and bands. *Figure 34* and *Figure 35* present rankings for inaccuracy and imprecision.

L1

3	4	1	2	5	
12	9	1	7	10	1
3	2	11	13	14	3
6	15	8	5	4	2

L2

4	3	1	2	5	
9	6	1	5	14	1
3	2	7	4	15	2
13	11	8	10	12	3

L3

5	3	4	1	2	
13	5	10	7	4	1
8	3	15	12	11	2
9	14	2	6	1	3

X1

3	1	2	
5	6	13	5
11	4	10	1
14	1	7	3
15	3	8	4
12	2	9	2

X2

2	1	3	
9	4	7	2
5	11	14	4
3	6	12	3
8	1	10	1
15	13	2	5

Figure 34. Inaccuracy ranking for L1, L2 and L3 (left), and for X1 and X2 (right).

L1

3	1	4	2	5	
8	5	7	3	15	2
6	2	4	1	11	1
12	10	13	9	14	3

L2

3	1	5	2	4	
6	4	11	5	9	2
3	1	8	2	7	1
13	12	15	10	14	3

L3

4	2	5	1	3	
10	7	9	3	6	2
8	2	5	1	4	1
14	11	15	12	13	3

X1

3	2	1	
11	9	10	1
13	8	6	3
14	5	1	4
15	7	3	5
12	2	4	2

X2

2	3	1	
12	15	13	5
10	14	8	4
5	9	7	1
4	11	3	2
1	6	2	3

Figure 35. Imprecision ranking for L1, L2 and L3 (left), and for X1 and X2 (right).

Insights. A key observation is that sequence is not consistent for inaccuracy and imprecision. Hence, region and band inaccuracy and imprecision can be independent from one another. Rankings and proportions each have their uses. Rankings can point out regions of interest but they do not indicate of the extent of inaccuracy or imprecision.

6.4.8. Circumferential and Axial Directionalities

Figure 36 compares the significance of the orthogonal spatial dimensions, i.e. the circumferential versus axial dimensions, which applies to inaccuracy and imprecision reflecting bias or variability around the cylinder or across its axis.

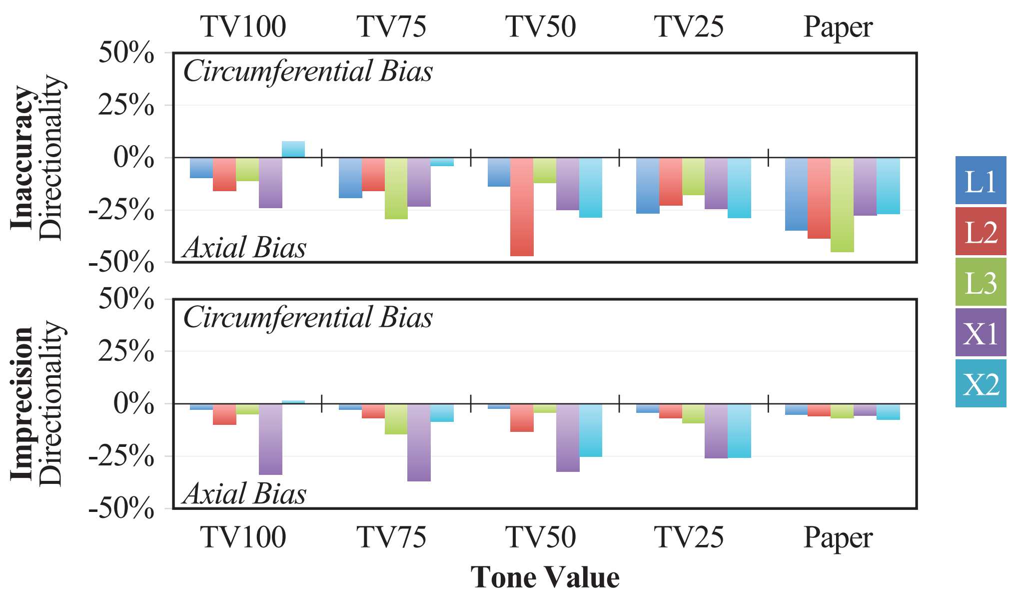

Figure 36. Directionalities for inaccuracy (top) and imprecision (bottom).

6.5. Visualization and Interpretation of Printing Uniformity

6.5.1. Visualization of Inaccuracy

This section provides comparative analysis of inaccuracy between pressruns focusing on key solid-ink uniformity metrics in comprehensive and intuitive figures. Complete tables and figures covering the entire set of metrics for all the pressruns and all the tone levels are provided in the appendix.

Electrophotography Pressruns. X1 and X2 exhibit very different inaccuracy trends. X1 has a significantly higher overall inaccuracy score ($v\Delta^{X1}=-473\%$) compared to X2 ($v\Delta^{X2}=-174\%$) relative to the standard aim (1.68±0.05 D). A visual summary of the inaccuracy for the two pressruns is shown in *Figure 37*.

Figure 37. Inaccuracy scores at TV100 for X1 (Left) and X2 (Right).

X1 exhibits higher region inaccuracy ($v\delta^{X1}_{r\,avg}=-49.1\%$) than X2 ($v\delta^{X2}_{r\,avg}=-17.8\%$). Circumferentially, X1 and X2 are comparable ($v\delta^{X1}_{c\,avg}=-14.4\%$; and, $v\delta^{X2}_{c\,avg}=-13.6\%$). Axially, X1 exhibits higher inaccuracy ($v\delta^{X1}_{a\,avg}=-49.3\%$) than X2 ($v\delta^{X2}_{a\,avg}=-12.3\%$).

X1 circumferential and axial inaccuracy scores differ largely in favor of the latter direction whereas X2 shows very little score difference. Inherently, X1 has a more pronounce axial bias as indicated by the inaccuracy directionalities ($d\delta^{X1}_{ca}$=C3:A7) whereas X2 has more stable bias towards the circumferential direction ($d\delta^{X2}_{ca}$=C6:A4).

Lithography Pressruns. L1, L2 and L3 exhibit many similarities. L1 has the highest run inaccuracy score ($v\Delta^{L1}=-215\%$) compared to L2 and L3 ($v\Delta^{L2,L3}=-192\%$) relative to the standard (1.68±0.05 D). Visual inaccuracy summaries are shown in *Figure 38*.

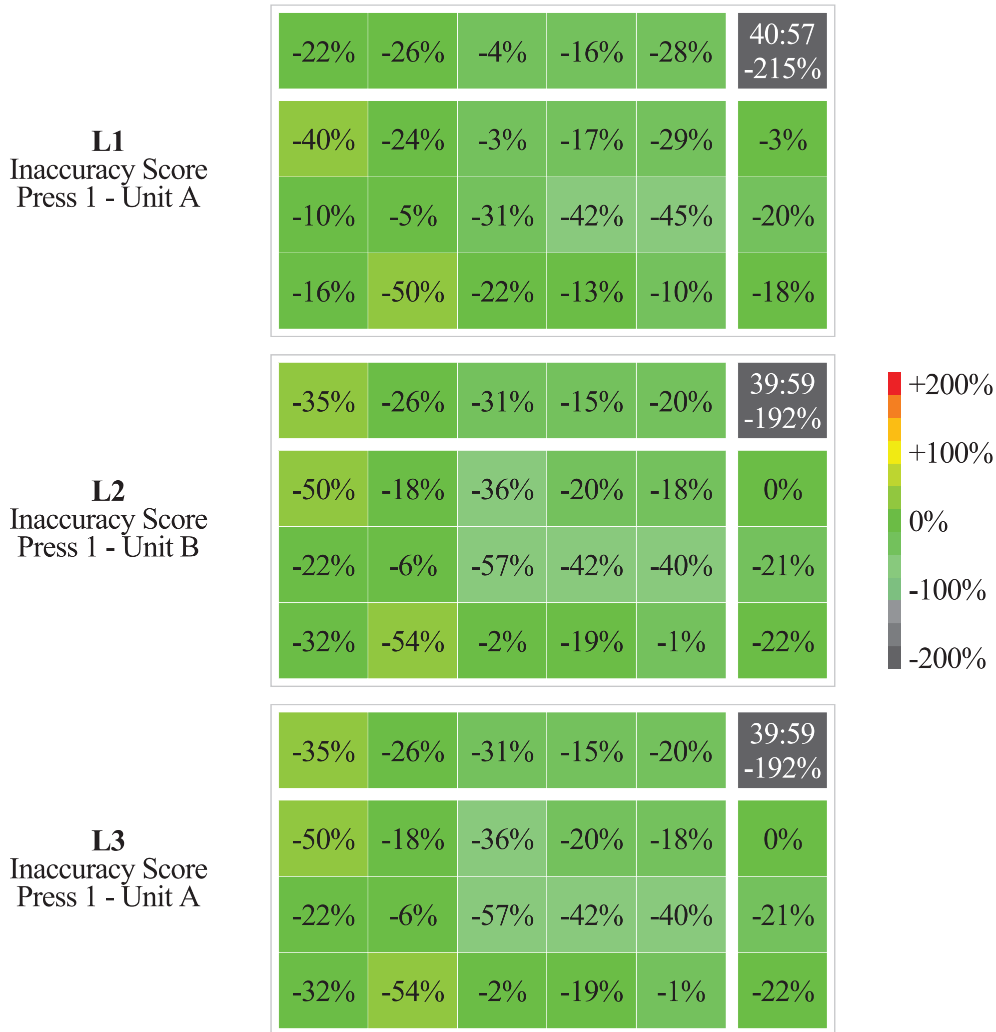

Figure 38. Inaccuracy scores at TV100 for L1 (Top), L2 (Middle) and L3 (Bottom).

L2 exhibits higher region inaccuracy ($v\delta^{L2}_{r\,avg}=-36.1\%$) than L3 ($v\delta^{L3}_{r\,avg}=-27.8\%$) and L1 ($v\delta^{L1}_{r\,avg}=-23.8\%$). Circumferentially, L2 is higher ($v\delta^{L2}_{c\,avg}=-17.7\%$) than L3 ($v\delta^{L3}_{c\,avg}=-14.3\%$) and L1 ($v\delta^{L1}_{c\,avg}=-13.7\%$). Axially, L2 is higher ($v\delta^{L2}_{a\,avg}=-29.6\%$) followed by L3 ($v\delta^{L3}_{a\,avg}=-25.4\%$) and L1 ($v\delta^{L1}_{a\,avg}=-19.2\%$).

Circumferential and axial inaccuracy scores for all lithography runs differ largely in favor of the latter. Inherently, they all have more pronounce axial bias, as indicated by the inaccuracy directionalities, where L2 shows higher axial bias ($d\delta^{L2}_{c:a}$=C3:A7) than the slightly lower bias for L1 and L3 ($d\delta^{L1,L3}_{c:a}$=C4:A6).

6.5.2. Visualization of Imprecision

This section provides comparative analysis of imprecision between pressruns focusing on key solid-ink uniformity metrics in comprehensive and intuitive figures. Complete tables and figures covering the entire set of metrics for all the pressruns and all the tone levels are provided in the appendix.

Electrophotography Pressruns. X1 and X2 exhibit very different imprecision trends. X1 has a significantly high run imprecision score ($v\mathrm{K}^{X1}=-233\%$) compared to X2 ($v\mathrm{K}^{X2}=-148\%$) relative to the standard tolerance (±0.05 D). A visual summary is shown in *Figure 39*.

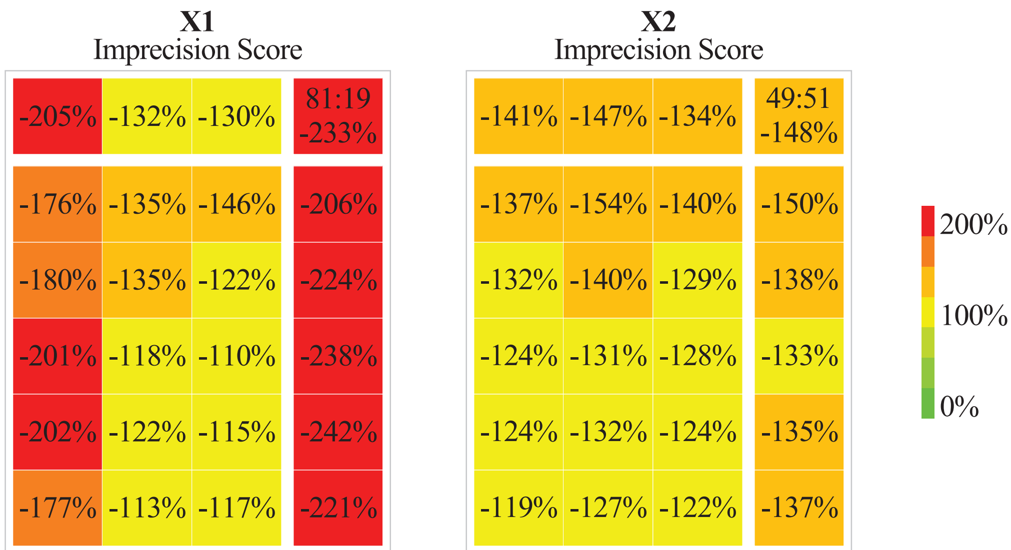

Figure 39. Imprecision scores at TV100 for X1 (Left) and X2 (Right).

X1 and X2 exhibit similar mean region imprecision ($v\kappa^{X1}_{r\,avg}=-144.6\%$; and, $v\kappa^{X2}_{r\,avg}=-130.9\%$), notwithstanding the substantially different spread. X1 exhibits higher circumferential imprecision ($v\kappa^{X1}_{c\,avg}=-226.3\%$; and, $v\kappa^{X1}_{a\,avg}=-155.7\%$), and X2 exhibits equivocal circumferential and axial imprecision ($v\kappa^{X2}_{c\,avg}=-138.6\%$; and, $v\kappa^{X2}_{a\,avg}=-140.7\%$).

Circumferential and axial imprecision scores differences translate into observable axial bias for X1 and no observable directionality bias for X2. Inherently, X1 exhibits a bias for the axial direction ($d\kappa^{X1}_{c:a}$=C3:A7) and X2 exhibits no bias ($d\kappa^{X2}_{c:a}$=C5:A5).

X1 exhibits higher unevenness ($f\kappa_{T:E}^{X1}$=T19:S81) whereas X2 exhibits equivalent unevenness and unrepeatability ($f\kappa_{T:E}^{X2}$=T55:S45). A visual breakdown of the spatial-temporal imprecision is shown in *Figure 40*.

X1
Imprecision Factors

-205% **26:74**	-132% **48:52**	-130% **54:46**	-233% **19:81**
-176% **37:63**	-135% **47:53**	-146% **52:48**	-206% **27:73**
-180% **39:61**	-135% **59:41**	-122% **69:31**	-224% **24:76**
-201% **25:75**	-118% **53:47**	-110% **63:37**	-238% **17:83**
-202% **27:73**	-122% **57:43**	-115% **67:33**	-242% **18:82**
-177% **30:70**	-113% **56:44**	-117% **60:40**	-221% **19:81**

X2
Imprecision Factors

-141% **57:43**	-147% **62:38**	-134% **62:38**	-148% **55:45**
-137% **63:37**	-154% **61:39**	-140% **61:39**	-150% **57:43**
-132% **77:23**	-140% **77:23**	-129% **75:25**	-138% **72:28**
-124% **75:25**	-131% **80:20**	-128% **71:29**	-133% **70:30**
-124% **72:28**	-132% **73:27**	-124% **71:29**	-135% **64:36**
-119% **65:35**	-127% **70:30**	-122% **64:36**	-137% **54:46**

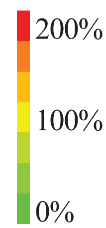

Figure 40. Spatial-temporal imprecision factors for X1 (Left) and X2 (Right).

X1 unevenness tends to increase at the driver side where imprecision is highest and substantially diminish in favor of higher unrepeatability towards the operator side. X2 unrepeatability is highest at the center of the sheet and tends to decrease slightly but remains higher than unevenness indicating spatially uniform output.

Lithography Pressruns. L1, L2 and L3 exhibit many similarities. L2 has the highest run imprecision score (vK^{L2} =−236%) followed by L1 (vK^{L1} =−199%) and L3 (vK^{L3} =−192%) relative to the standard tolerance (±0.05 D). A visual summary is shown in *Figure 41.*

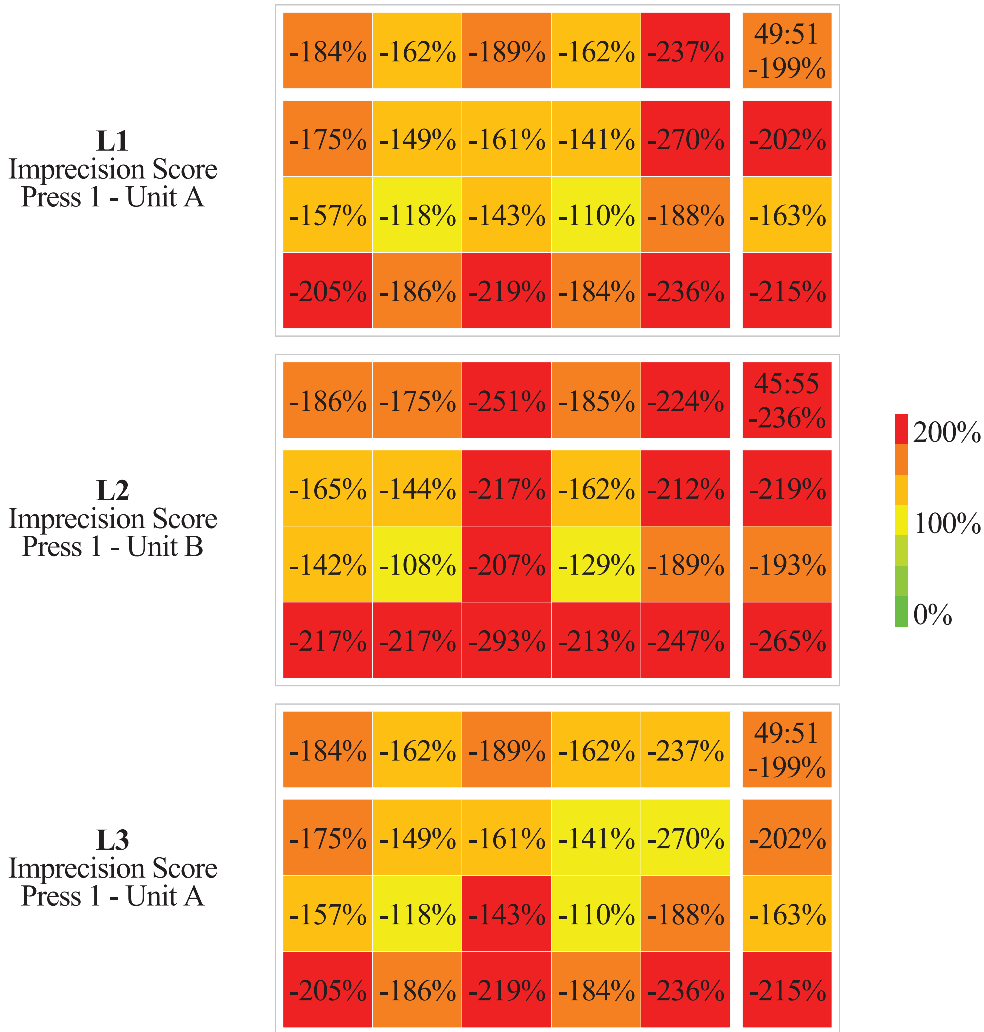

Figure 41. Imprecision scores at TV100 for L1 (Top), L2 (Middle) and L3 (Bottom).

L2 exhibits higher region imprecision ($v\kappa_{r\,avg}^{L2}$ =−190.8%) than L1 ($v\kappa_{r\,avg}^{L1}$ =−176.1%) and L3 ($v\kappa_{r\,avg}^{L3}$ =−160.7%). Circumferentially, L2 is higher ($v\kappa_{c\,avg}^{L2}$ =−204.2%) than L1 ($v\kappa_{c\,avg}^{L1}$ =−186.8%) and L3 ($v\kappa_{c\,avg}^{L3}$ =−175.4%). Axially, L2 is also higher ($v\kappa_{a\,avg}^{L2}$ =−204.2%) followed by L1 ($v\kappa_{a\,avg}^{L1}$ =−193.3%) and L3 ($v\kappa_{a\,avg}^{L3}$ =−182.7%).

L2 has negligible axial imprecision directionality bias ($d\kappa_{c:a}^{L2}$ =C4:A6) next to L1 and L3 ($d\kappa_{c:a}^{L1,L3}$ =C5:A5). L1 and L2 exhibit critical axial hotspots along the operator side, and L2 at the center. L1, L2, and L3 exhibit circumferential hotspots across the lead edge.

All runs exhibit more unevenness, highest for L2 ($f\kappa^{L2}_{T:E}$ =15:85) and L3 ($f\kappa^{L3}_{T:E}$ =16:84) and lower for L1 ($f\kappa^{L1}_{T:E}$ =24:76). A visual breakdown is shown in *Figure 42*.

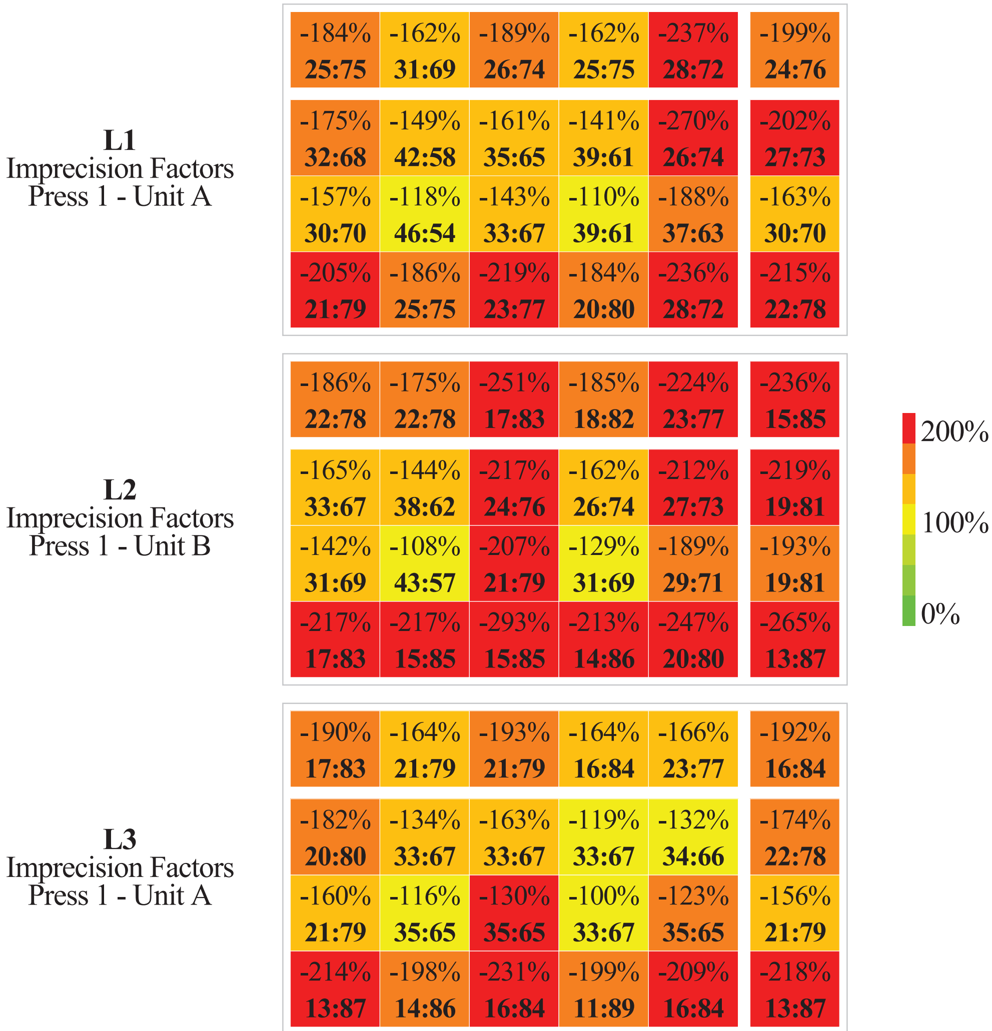

Figure 42. Spatial-temporal imprecision factors for L1 (Top), L2 (Middle) and L3 (Bottom).

Unevenness contribution factors within the regions for L1, L2 and L3 tend to increase with increasing imprecision. Inherently, it may be inferred that unrepeatability is more consistent than unevenness, where the latter tends to increase in the previously indicated hotspot regions.

Chapter 7
Summary and Conclusions

This study looks into the benchmarking and evaluation of the uniformity of printing systems relative to standard industry tolerances. It proposes a set of device- and process-independent spatial and temporal uniformity metrics. A number of concepts were consolidated and refined from existing literature in a comprehensive conceptual framework. This framework defines indicators that are used to formalize practical metrics through statistical analysis of the central tendencies and variances of printing density.

7.1. Summary

The primary contributions of this study are the development of the set of metrics and testing methods that may help in further developments of standards, quality control systems, and, benchmarking new printing technologies that are penetrating the markets.

The conceptual framework incorporates the various concepts from the top-level dimensions (i.e., accuracy and precision) down to indicators. It was a necessary precursor to developing practical metrics that tie directly to clearly defined indicators. As such, the framework may prove valuable to other interested scholars and researchers in overcoming the lack of seminal work and the limited range of isolated works on the topic.

The data collected and used in this study also offers value for future research. This data was used for refining and testing the validity of the proposed indicators and metrics. The sample incorporates spectrophotometric data for solids, quartertones (i.e., 25%, 50% and 75%) and paper throughout the printing plane. Five pressruns were conducted on three presses at high spatial resolution. Each dataset includes data for 56-57 sheets from 200 consecutive impressions using sequential and quasi-random sampling.

Finally, a number of data visualization techniques are used to help distill the data from the test runs. These aids were essential to completing the analysis and presenting results and findings in *Chapter 6*. The results and findings provide a basic template for systematic reporting on the uniformity of printing systems in future studies.

The following sections provide highlights and concluding notes for each of the components mentioned. The reader is referred to the respective chapters for specifics.

7.1.1. Conceptual Framework

The conceptual framework addresses the accuracy and precision dimensions of printing uniformity. Each dimension encompasses indicators within constructs for run and regional uniformity, shown in *Figure 13 (pp. 34)* repeated below.

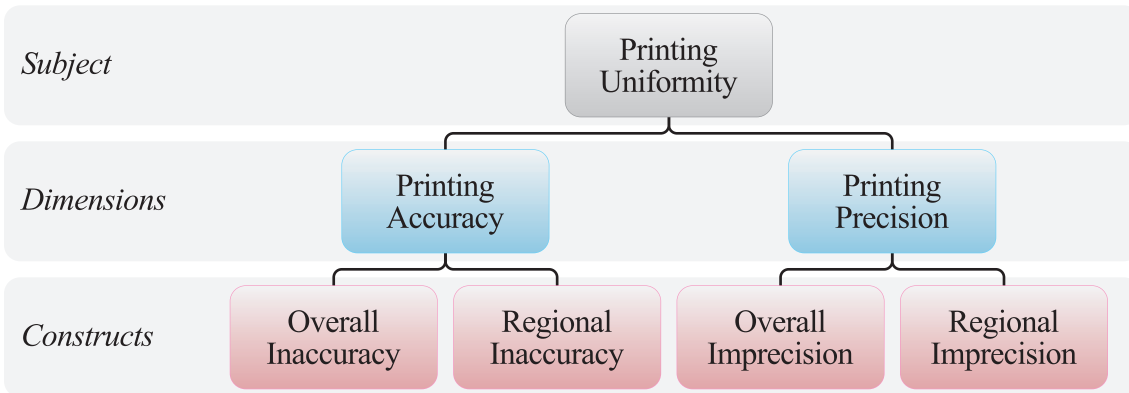

Figure 13 (repeated). Printing accuracy and precision constructs.

Indicators include run and regional scores, region contribution proportions, unevenness and unrepeatability factors, and, circumferential and axial directionality ratios, shown in *Figure 14 (pp. 34)* repeated below.

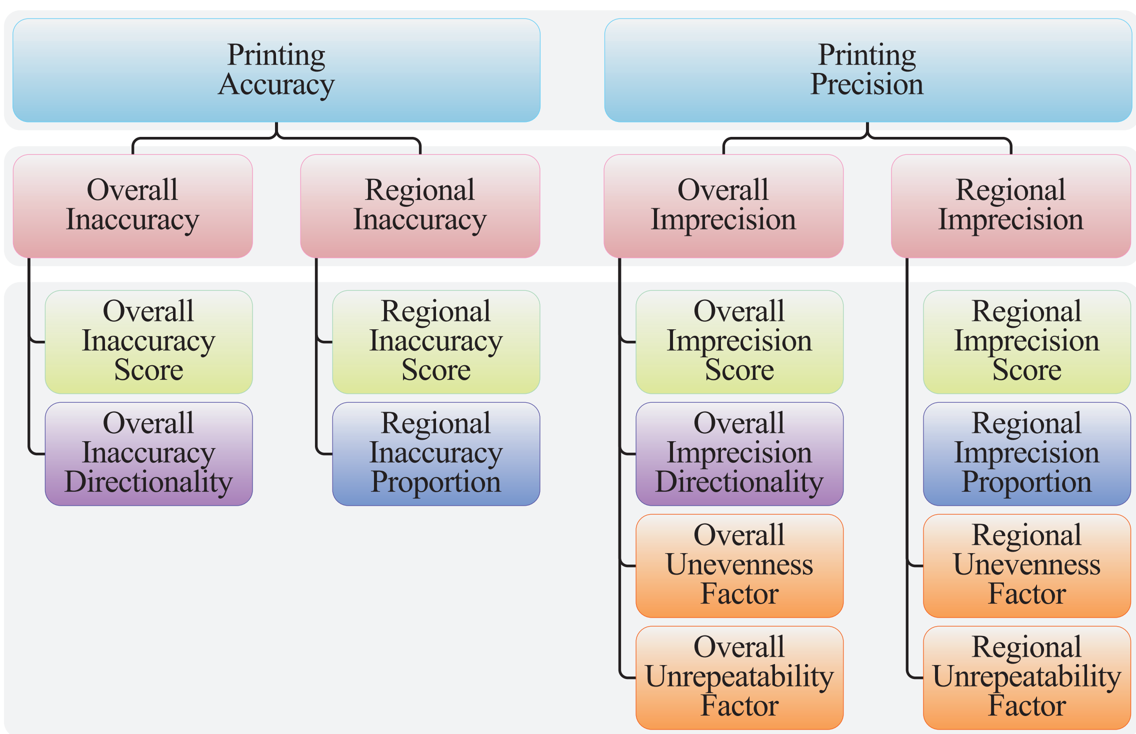

Figure 14 (repeated). Overall versus sheet, region, and, band spatial subsets.

7.1.2. Qunatitative Models

The proposed metrics address various aspects of accuracy and precision based on systematic sampling of the printing plane across a number of sheets. The reader is referred to section *4.1* for the following equations as indicated.

Scores are computed for the relative inaccuracy (relative to the mean of the run) and imprecision of regions of interest and absolute inaccuracy (relative to a standard aim point) and imprecision for the entire printing plane; refer to *Equation 1* through *Equation 8*. Regional proportions are computed relative to the cumulative sum of inaccuracy and imprecision of the entire set of uniformly divided regions; refer to *Equation 9* and *Equation 10*. Run directionality ratios are computed relative to the cumulative sum of inaccuracy and imprecision for circumferential and axial directionality bands; refer to *Equation 16* and *Equation 17*. Spatial-temporal factors are computed relative to the sum of the squares of variances for sheets (variance between patches in each sheet) and for patches (variance between sheets for each patch), respectively; refer to *Equation 11* through *Equation 15*.

7.1.3. Testing Methods

The design test form used for fingerprinting has to be adapted to the dimensions of the press and the chart specifications of the automated spectrophotometer. Sampling constraints also need to be adjusted for in the design, i.e. alignment of test blocks with ink keys in offset. Instruments constraints are also taken into consideration, i.e. maximum chart dimensions and track marks placement. The final design can contain more than one test chart, as is necessary for the offset press used here. Each chart contains a 4 × 4 repeating checkerboard target blocks, shown in *Figure 16 (pp. 46)*, containing 8 solid, 2 three-quartertone, 2 midtone, 2 quartertone, 1 paper, and, 1 slur-doubling patch. For the presses tested, the total patch count for the landscape offset press is 3744, divided on 2 charts, and, the total count for the portrait electro-photographic presses is 2992 in 1 chart.

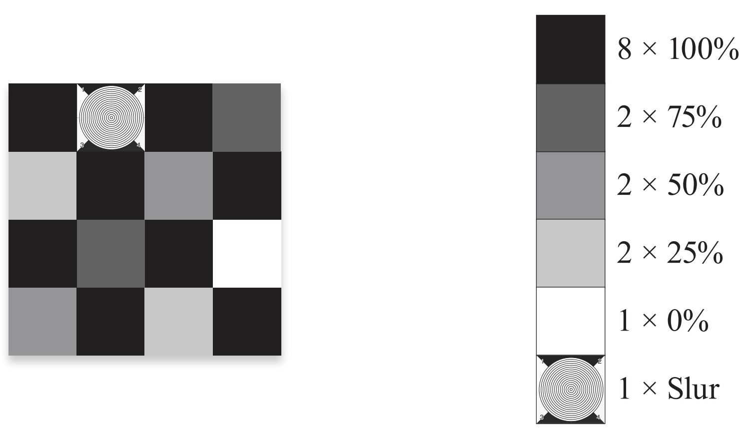

Figure 16 (repeated). 16-Patch Checkerboard Test Target Repeating Block (4×4)

The sheets are measured using an i1 iSis automated spectrophotometer using a special MatLab software used to structure the measuring and data storage process to eliminate human error from redundancy. The software stores 36-point spectral reflectance data for every patch on every chart and stores the positioning in mapping table, as well as, additional metadata included target specifications, prepress workflow, consumables, printing, sample selection, measurement and instrument information.

7.1.4. Pressruns & Results

Five pressruns were conducted on 1 lithographic and 2 electrophotographic presses. The procedure for each run includes: 1) designing the test form, 2) generate plates when applicable, 3) cleanup and loading the ink and paper, 4) make-ready till okay sheet, 5) printing a 200 sheet buffer after first okay sheet, and, 6) printing 300 sheets for sample selection. Sample sheets are selected from within 200 consecutive prints (from the 300 sheets) by taking: 1) the first 10 sequential sheets, 2) a sheet for every 5 quasi-random sheets (taken at random) between sheets 11 and 190, and, 3) the last 10 sequential sheets.

Printing accuracy was analyzed for solids and tints relative to standard aims and tolerances. More comprehensive results for solids are presented which compare the electrophotography runs (X1 and X2) and the lithography runs (L1, L2 and L3). X1 (newer model than X2) shows high overall inaccuracy ($v\Delta^{\mathrm{X1}}=-473\%$), with a strong axial bias ($d\delta_{c:a}^{\mathrm{X1}}=$C3:A7) between the sides. X2 shows less overall inaccuracy ($v\Delta^{\mathrm{X2}}=-174\%$), with some circumferential bias ($d\delta_{c:a}^{\mathrm{X2}}=$C6:A4) from lead edge to tail. L1 and L3 (same printing unit) show inconsistent overall inaccuracy ($v\Delta^{\mathrm{L1}}=-215\%$ and $v\Delta^{\mathrm{L3}}=-192\%$), with consistent axial bias ($d\delta_{c:a}^{\mathrm{L1,L3}}=$C4:A6). L2 (separate unit) exhibited overall inaccuracy ($v\Delta^{\mathrm{L2}}=-192\%$) similar to L3, with stronger axial bias ($d\delta_{c:a}^{\mathrm{L2}}=$C3:A7), which is comparable to X1 directional bias.

Printing precision was also analyzed for solids and quartertones relative to standard tolerances. Comprehensive results for solids also are presented. X1 shows high overall imprecision ($v\mathrm{K}^{\mathrm{X1}}=-233\%$), with relatively low regional imprecision ($v\kappa_{r\,\mathrm{avg}}^{\mathrm{X1}}=-144.6\%$) suggesting imprecision hotspots. X2 shows less overall imprecision ($v\mathrm{K}^{\mathrm{X2}}=-148\%$), with closely related regional imprecision ($v\kappa_{r\,\mathrm{avg}}^{\mathrm{X2}}=-130.9\%$) suggesting distributed spatial patterns. L1 and L3 show similar overall imprecision ($v\mathrm{K}^{\mathrm{L1}}=-199\%$ and $v\mathrm{K}^{\mathrm{L3}}=-192\%$), and closely related regional imprecision ($v\kappa_{r\,\mathrm{avg}}^{\mathrm{L1}}=-176.1\%$ and $v\kappa_{r\,\mathrm{avg}}^{\mathrm{L3}}=-160.7\%$). L2 shows higher overall imprecision ($v\mathrm{K}^{\mathrm{L2}}=-236\%$), with equivocal regional imprecision ($v\kappa_{r\,\mathrm{avg}}^{\mathrm{L2}}=-204.2\%$) to L1 and L3, with consideration to L2's higher overall imprecision. X2 shows slight temporal imprecision bias ($f\kappa_{\mathrm{T:E}}^{\mathrm{X2}}=$T55:S45) while all others show higher spatial bias ($f\kappa_{\mathrm{T:E}}^{\mathrm{X1}}=$T19:S81, $f\kappa_{\mathrm{T:E}}^{\mathrm{L1}}=$24:76, $f\kappa_{\mathrm{T:E}}^{\mathrm{L2}}=$15:85 and $f\kappa_{\mathrm{T:E}}^{\mathrm{L3}}=$16:84), which indicates more unevenness than unrepeatability.

7.2. Conclusions

This study primarily concludes that the topic of printing uniformity requires the attention of the research community due to its implications on quality control applications and standardization efforts and due to the limited range of works on the topic.

Tremendous effort is invested by the industry to improve how we measure and control variability on the press. ISO standards and industry specifications provide comprehensive schemas for process control. However, there is a limitation due to heavy reliance on an essential premise; that for any press, measuring density using proxy color bars is effective to ensure the conformance of the actual printed image.

Research on printing uniformity did not yield a reliable consensus on any constructs, indicators, metrics, and, testing methods. This work is an effort to reconcile these different aspects and build bridges between many existing islands of research, to propose concepts, metrics and methods that harmonize prior efforts by several authors.

There is much to be gained from the insights encountered during the course of exploring printing uniformity. Trying to understand how to measure and represent the uniformity of presses or other phenomena requires an agile three-tiered approach of iteratively devising the conceptual framework, models and testing methods.

Surprisingly enough, in the of case of this study, the testing method was in fact finalized while in the first iterations of devising the framework and metrics. Data collection required only abstract and superficial understanding of the dimensions and constructs that would be incorporated in the framework. Thus, data for exploring printing uniformity starts and ends with adequate sampling of ink density throughout the printing plane (spatially), and, across sheets and between runs (temporally). The data should offer contrasting features or treatments, i.e., various printing processes and press units.

7.2.1. Future Work

The contributions made here can be adapted to explore the uniformity of other attributes in print. They may also be adopted in completely different applications where there is a need for analyzing spatial-temporal variability. In general terms, this work can be adopted for any form of statistical analysis for the weighted significance of orthogonal dimensions. And finally, this work can serve as template for exploring phenomena using the three-tiered approach for devising the concepts, models and methods.

Future research on the uniformity of various printing systems across processes may improve our understanding of printing uniformity. Comprehensive testing across systems and processes creates opportunities for testing standing assumptions for the continued improvement of quality control practices to achieve higher color consistency.

Bibliography

Abdel Motaal, S. A., & Sikander, M. (2009). Repeatability of Ink Transfer and Color Management in Lithography. *TAGA Proceedings*, (pp. 512-537). New Orleans.

Babbie, E. (2011). *The Basics of Social Research* (5th Edition ed.). (E. Mitchell, D. Moneypenny, A. Parkins, R. Krapf, & M. Cregger, Eds.) Belmont, CA, USA: Wadsworth.

Breede, M. (2007). The Effect of Ink Film Thickness Variations on Color Control in the Circumferential Printing Cylinder Direction of Offset Presses. *TAGA Proceedings*, (pp. 63-78). San Francisco.

Eerola, T., Lensu, L., Kälviäinen, H., Kamarainen, J. K., Leisti, T., Nyman, G., et al. (2010). Full Reference Printed Image Quality: Measurement Framework and Statistical Evaluation. *Journal of Imaging Science and Technology , 54* (1).

IDEAlliance. (2007). GRACoL® 7 Specification for Commercial Printing on a #1 Coated Sheet . *7*.

ISO. (2007). Graphic technology — Process control for the manufacture of half-tone colour separations, proof and productions prints — Part 7: Off-press proofing process working directly from digital data . *12647-7* .

ISO. (2004). Graphic technology — Process control for the production of half-tone colour separations, proof and production prints — Part 2: Offset lithographic processes . *12647-2 , 2*.

ISO. (2007). Graphic technology — Process control for the production of half-tone colour separations, proof and production prints — Part 2: Offset lithographic processes (Amendment 1). *12647 , 2*.

ISO. (2011). Graphic technology — Requirements for printed matter utilizing digital printing technologies for the commercial and industrial production — Part 1: Parameters and measurement methods.

ISO. (2009). Graphic technology — Vocabulary — Part 3: Printing terms. *12637-3 , 1*.

ISO. (2012, 03 27). Information Technology—Office equipment — Measurement of image quality attributes for hardcopy output — Monochrome text and graphic images.

Jabareen, Y. R. (2009). Building a Conceptual Framework: Philosophy, Definitions, and Procedure. *International Journal of Qualitative Methods , 8* (4), 49-62.

Khullar, S. (2010). *Automatic Multi-Resolution Spatio-Frequency Mottle Metric (SFMM) for Evaluation of Macrouniformity.* Master's Thesis, Rochester Institute of Technology, Department of Electrical & Microelectronics Engineering, Rochester.

Kraushaar, A. (2013). *Image Quality Research at Fogra* . Presentation, International Standards Organization, Technical Committee 130 Joint Working Group 14, San José.

NPES. (2007). *CGATS — Color Characterization Data Set Development — Analysis and Reporting.* Technical Report.

NPES. (2003). *CGATS — Color Characterization Data Set Development — Press Run Guidelines.* Technical Report.

NPES. (2007). *CGATS — Color Characterization Data Set Development — Procedures for Color Measurement System Process Control and Inter-lab Coordination.* Technical Report.

Oakes, T., Sossi, V., & Ruth, T. (1997). Normalization in 3D PET: Comparison of Detector Efficiencies Obtained from Uniform Planar and Cylindrical Sources. *IEEE Medical Imaging Conference.*

Ploumidis , D. M. (2007). A Quantitative and Qualitative Assessment of the Impact of the Number of Patches Included in Profiling Targets. *TAGA Proceedings* (pp. 383-402). San Francisco: Printing Industries of America.

Radencic, G., Neumann, E., & Bohan, M. (2008). Spectrophotometer inter-instrument agreement on the color measured from reference and printed samples . *TAGA Proceedings*, (pp. 232-251).

Rasmussen, D. R., Donohueb, K. D., Ngc, Y. S., Kressd, W. C., Gaykemae, F., & Zoltner, S. (2006). ISO 19751 Macro-Uniformity. In L. C. Cui, & Y. Miyake (Ed.), *SPIE-IS&T Electronic Imaging*, *6059.*

Rech, H. (2010). *Untersuchung des dynamischen Verhaltens ausgesuchter Konfigurationen eines Modellfarbwerkes.* Retrieved 08 15, 2010, from VDD: http://www.vdd-net.de/Publikationen/Rech/Farbwerksuntersuchungen.html

Seymour, J. (2008). Building a Bridge from Dense City to Colorimetropolis. *TAGA Proceedings.*

Sigg, F. (2007). Spatial Uniformity of Offset Printing. *TAGA Proceedings*, (pp. 649-658). San Francisco.

Siljander, R., & Fisch, R. (2001). Accuracy and Precision in Color Characterization. *TAGA Proceedings*, (pp. 57-78).

X-Rite. (2007, 07 12). Eye-One iSis Chart Design Guidelines. *2*.